An appraisal using magnetic data of the Continent to Ocean Transition Structure West of Iberia

Marta Neres[1,2], César R. Ranero[3,4]

[1] IPMA - Instituto Português do Mar e da Atmosfera, 1749-077 Lisboa, Portugal

[2] IDL - Instituto Dom Luiz, Universidade de Lisboa, 1749-016 Lisboa, Portugal

[3] ICM-CSIC - Consejo Superior de Investigaciones Científicas, Instituto de Ciencias del Mar, 08003 Barcelona, Spain

[4] ICREA -Institució Catalana de Recerca i Estudis Avançats, 08010 Barcelona, Spain

Corresponding author: Marta Neres (marta.neres@ipma.pt)

ORIGINAL UNEDITED MANUSCRIPT

Downloaded from https://academic.oup.com/gji/advance-article/doi/10.1093/gji/ggad163/7120036 by Universidade do Porto user on 18 April 2023

ABSTRACT

About half of the rifted margins purportedly formed by extension with minor magmatism. The conceptual models of those magma-poor systems are greatly influenced by the continent-to-ocean transition structure of the archetypal magma-poor West Iberia Margin. In the past, interpretation of magnetic data of West Iberia has been used to constrain conceptual rifting models, including the structure of the transition from the exhumed mantle domain to the oceanic crust formed at a spreading center. However, uncertainties on geophysical data were

© The Author(s) 2023. Published by Oxford University Press on behalf of The Royal Astronomical Society.

generally not considered leading to over-detailed interpretations. We use synthetic magnetic modelling to show that magnetic data acquired at sea-level cannot resolve sub-horizontal lithological layering in deep-water continental margins. We then present new magnetic modelling guided by a refined velocity model of the wide-angle seismic IAM-9 profile that shows that the magnetic J-anomaly correlates with oceanic crust that abuts exhumed mantle across a vertical boundary. This well-constrained observation supports that seafloor spreading initiated abruptly, terminating mantle exhumation. Conventional wisdom dictates that the sudden efficient melt extraction relates to a mechanical threshold during lithospheric thinning and concomitant asthenospheric upwelling under which melt can migrate toward the surface. However, our results support that mantle melting creating oceanic crust was probably not driven by gradual lithospheric thinning and asthenospheric upwelling, but by seafloor spreading center propagation that cut across the lithosphere, creating the abrupt structure.

KEYWORDS

- Composition and structure of the oceanic crust
- Magnetic anomalies: modelling and interpretation
- Magnetic properties
- Marine magnetics and palaeomagnetics
- Continental - margins: divergent
- Oceanic crust
- West Iberia margin
- Crustal break up

ORIGINAL UNEDITED MANUSCRIPT

Downloaded from https://academic.oup.com/gji/advance-article/doi/10.1093/gji/ggad163/7120036 by Universidade do Porto user on 18 April 2023

1. INTRODUCTION

Continental rifting causes lithospheric stretching and eventually the breakup of the crust. The late stages of crustal thinning, before full breakup and the formation of a conjugate pair of rifted margins, may have associated different volumes of magmatism. When final rifting is associated to comparatively large volume of magmatism, forming tens-of-km thick new crust, rifting is considered magma-rich like in the southern and northern Atlantic (e.g. White and McKenzie, 1989). Final breakup may also be associated to moderate magmatism yielding 5-8 km thick crust like in the South China Sea (Cameselle et al 2017), the Gulf of Lions (Merino et al., 2021), and the Tyrrhenian Basin (Prada et al., 2014). There is also a rifting process that occurs with crustal breakup with little or no magmatic activity associated, hence known as magma-poor rifting, causing the tectonic exhumation of the lithospheric mantle and it exposure at the seafloor at the time of extension. The amount of magmatism, its origin as synrift or early seafloor spreading and its significance in magma-poor rifting processes are still debated. The debate is partially triggered because exhumed mantle is serpentinised to several km depth, and as a result has seismic velocities and densities similar to magmatic rocks, which makes it difficult to unequivocally detect with geophysical methods several-km-thick igneous intrusions, and they have only been documented by drilling (Whitmarsh et al., 2001).

The West Iberia Margin (WIM) rift structure has fundamentally influenced developments of conceptual models of magma-poor lithospheric extension (Whitmarsh et al., 2001; Peron-Pinvidic et al., 2013; 2019; Haupert et al., 2016; Chenin et al., 2021). Drilling results in the Deep Galicia Margin, Iberia Abyssal Plain, and Gorringe Bank (Boillot et al., 1980; Sawyer et al.,

ORIGINAL UNEDITED MANUSCRIPT

Downloaded from https://academic.oup.com/gji/advance-article/doi/10.1093/gji/ggad163/7120036 by Universidade do Porto user on 18 April 2023

1994; Whitmarsh et al., 1998) and their extrapolation with geophysical methods (Discovery 215 Working Group, 1998; Dean et al., 2000; Sallarès et al., 2013; Merino et al., 2021a; Grevemeyer et al., 2022) mapped the structure of the continent-to-ocean transition (COT). Similar, albeit less extensive, studies have been done in the conjugate Newfoundland margin (Lau et al., 2006; Shillington et al., 2006; van Avendonk et al. 2006). However, the geological interpretation of the geophysical data sets remains disputed (Bronner et al., 2011; Nirrengarten et al., 2017; Manatschal et al., 2021; Chenin et al., 2021).

1.1. Open questions about the West Iberia Margin structure

The age and processes of the COT and initial seafloor spreading remain debated mainly because of the non-unique interpretation of some geophysical data sets concerning the nature of the crystalline rocks across the COT. Previous studies were not conclusive on the initial formation of oceanic crust, the presence of magmatic bodies within exhumed mantle (e.g. Russell and Whitmarsh, 2003), nor on the establishment of a steady-state spreading center (Whitmarsh et al., 2001; Nirrengarten et al., 2017). Moreover, the significance of mantle exhumation related to lithospheric extension and thinning, as well as the causes for termination of exhumation are disputed by contrasting models, with distinct implications for rift formation models. Mantle exhumation may have brought continental lithosphere to the surface (Boillot et al., 1980; Whitmarsh et al., 2001) or be related to ultra-slow seafloor spreading (Srivastava et al. 2000, Sibuet et al., 2007). Continental mantle exhumation is believed to end by either the gradual establishment of a steady-state spreading center, as the continental lithosphere extends and mantle melting progresses (Whitmarsh et al., 2001) or by

ORIGINAL UNEDITED MANUSCRIPT

Downloaded from https://academic.oup.com/gji/advance-article/doi/10.1093/gji/ggad163/7120036 by Universidade do Porto user on 18 April 2023

synrift magmatism unrelated to seafloor spreading (Bronner et al., 2011; Szameitat et al., 2020).

The interpretation of a subcontinental or slow-spreading affinity of mantle rocks drilled in the Iberia Abyssal Plain is a debate based on the interpretation of their radiogenic isotopic composition. Some studies claim that the peridotite refertilisation has a continental rifting origin because it is rare in abyssal oceanic peridotites (e.g. Müntener et al., 2009). However, a Variscan orogenic (e.g. Chazot et al., 2005) or oceanic origin (Rampone and Hofmann, 2012) of peridotite refertilization are also argued. Although West Iberia mantle contains plagioclase lherzolites (i.e. fertile rocks) that might indicate an exhumed continental mantle (Boillot et al., 1980), the conjugate Newfoundland exhumed mantle contains ultra-depleted refractory peridotite (Müntener & Manatschal, 2006) compositionally similar to refractory abyssal peridotites in mid-ocean ridges (Godard et al. 2008) and elsewhere (Warren, 2016). Ronda Peridotite shows the transformation of depleted continental mantle to fertile oceanic-like plagioclase lherzolites (Hidas et al., 2015) possibly associated to interaction with melts during late extension, a process recorded in other orogenic peridotites and proposed to occur also in COT settings (Varas-Reus et al., 2016).

Understanding the amount of continental lithospheric extension and the associated processes of mantle exhumation and magmatic production, and the locus of breakup of the WIM, is also essential for understanding the plate kinematics of Iberia and surrounding plates (Neres et al., 2012; 2013; Nirrengarten et al. 2017; 2018), the related regional rifting processes (Sandoval et al., 2019), the opening of the Bay of Biscay rift system, and the formation of the Pyrenees mountain chain (Sibuet el at., 2004; Vissers and Meijer, 2012; Barnett-Moore et al., 2016;

ORIGINAL UNEDITED MANUSCRIPT

Downloaded from https://academic.oup.com/gji/advance-article/doi/10.1093/gji/ggad163/7120036 by Universidade do Porto user on 18 April 2023

2017). However, many existing models are based on re-interpretation of vintage geophysical data, such as the compilation of shipborne magnetic data from the 1960s-80s (Verhoef et al., 1996) and crustal-scale Vp models based on sparse wide-angle data (Dean et al., 2000). Thus, different interpretations of the same geophysical data sets continue to be used to support competing models, often with little evaluation of their resolution and of the uncertainty in modelling approaches.

Magnetic lineations along the Iberia-Newfoundland conjugate system have been used to infer the structure and age of the crust, formation processes, and to calculate opening kinematics. Long discussed is the J-anomaly, a large-amplitude (>300 nT) magnetic anomaly that is well-defined south of the Azores-Gibraltar fracture zone at the oceanic lithosphere of the African plate (Tucholke and Ludwig, 1982; Rovere et al., 2004), but questioned in terms of origin and age in the WIM (Sibuet el at., 2004; Bronner et al., 2011; Nirrengarten et al., 2017; Szameitat et al., 2020). The IAM-9 seismic transect (Figure 1) has been repeatedly modeled to obtain the seismic velocity on the Iberia Abyssal Plain (Dean et al., 2000; Minshull et al., 2014; Grevemeyer et al., 2022), and its velocity structure has been used to guide the modelling of the magnetic structure of the crust (Bronner et al., 2011; Szameitat et al., 2020). These modelling results have been interpreted to discuss the processes of continental crust breakup, the formation of the COT, and the kinematics of the early opening of Iberia and Newfoundland (e.g. Bronner et al., 2011; Stanton et al., 2016; Nirrengarten et al., 2017; 2018; Szameitat et al., 2020). These interpretative models of the IAM-9 transect have been key to develop conceptual magma-poor rifting models (e.g. Peron-Pinvidic et al., 2013; 2019; Tugend et al., 2020; Haupert et al., 2016). Thus, the origin of the J-anomaly has been a key constraint for the

ORIGINAL UNEDITED MANUSCRIPT

Downloaded from https://academic.oup.com/gji/advance-article/doi/10.1093/gji/ggad163/7120036 by Universidade do Porto user on 18 April 2023

development of WIM formation models, which in turn are commonly translated into conceptual models of magma-poor rifting.

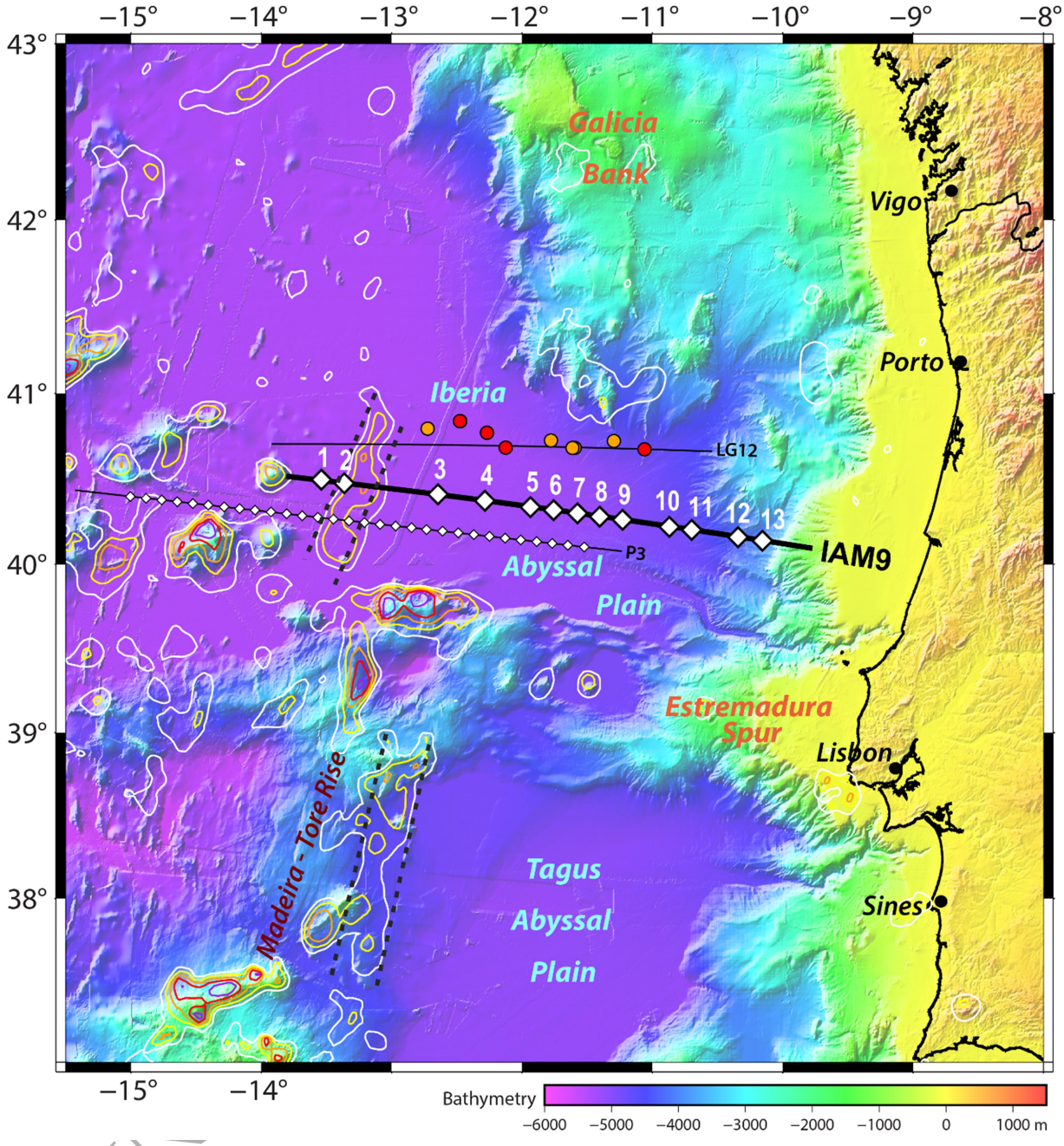

Figure 1. *Bathymetric map of the West Iberia Margin with the track of the IAM-9 wide-angle seismic line and Ocean Bottom Seismometer (OBS) locations (white diamonds). The tracks of*

ORIGINAL

Downloaded from https://academic.oup.com/gji/advance-article/doi/10.1093/gji/ggad163/7120036 by Universidade do Porto user on 18 April 2023

the Lusigal-12 (LG12) and FRAME-P3 (P3) seismic profiles are also shown. Main positive magnetic anomalies (Verhoef et al., 1996) are shown as coloured contours: 100 nT (white); 200 nT (yellow); 300 nT (orange); 400 nT (red); 500 nT (purple); black dashed lines highlight the J-anomaly. Red and orange dots are ODP drill sites of legs 149 and 173, respectively.

1.2. Challenges determining the basement structure with magnetic modeling

There have been several modelling attempts to decipher the transition from mantle exhumation to the first magmatic crust, integrating geophysical data sets across the J-anomaly magnetic data in the Iberia Abyssal Plain (Russell and Whitmarsh 2003; Bronner et al. 2011). New wide-angle seismic data collected across the Tagus Abyssal Plain with closely spaced ocean bottom seismometers (OBS) and coincident deep penetration seismic images (Merino et al., 2021a) indicates a basement structure more complex than previously detected with low-resolution wide-angle seismic data, making magnetic modelling based on previous low-resolution seismic velocity models (Afilhado et al., 2008) unlikely to represent the complex structure.

In the Iberia Abyssal Plain, similar closely spaced OBS wide-angle seismic data indicate an abrupt transition from exhumed mantle to oceanic crust (Grevemeyer et al., 2022; P3 in Figure 1). This structure is rather different from previous models produced along IAM-9 (Russell and Whitmarsh 2003; Bronner et al. 2011), which have been partially based on geological re-interpretation of the wide-angle velocity model of Dean et al. (2000) to infer the location of

ORIGINAL UNEDITED MANUSCRIPT

Downloaded from https://academic.oup.com/gji/advance-article/doi/10.1093/gji/ggad163/7120036 by Universidade do Porto user on 18 April 2023

magnetic sources in the basement. Interestingly, these works propose rather contrasting geological models: Bronner et al. (2011) proposed that J-anomaly is not a seafloor spreading anomaly, whereas Russell and Whitmarsh (2003) had proposed that seafloor spreading initiated before J-anomaly formation. Both models along IAM-9 contrast with the results of Grevemeyer et al (2022) along the new FRAME-P3 seismic line some 30 km to the south (Figure 1) that support the magnetic J-anomaly indeed as the first seafloor spreading anomaly.

In this work, we evaluate previous models of the WIM structure that integrate coincident shipborne magnetic data and seismic velocity models. We first show that some suffer from methodological and conceptual issues, and later we re-evaluate the available data to provide quantitative constraints that yield a more realistic geological model of the nature of the J-anomaly. These new constrains are important for a new understanding of the WIM and Newfoundland conjugate margins and have implications for conceptual magma-poor rift evolution.

2. METHODOLOGY

The magnetic anomaly caused by a magnetisation distribution $\vec{M}$ is expressed as:

$$\vec{B}\left(\vec{r}\right) = -\frac{\mu_0}{4\pi}\nabla_r \int_V \vec{M}\left(\vec{s}\right).\nabla_s\left(\frac{1}{\left|\vec{r}-\vec{s}\right|}\right)dV \qquad \text{(Equation 1)}$$

where $\vec{r}$ is the vector to the observation point and $\vec{s}$ varies within the source volume V (Blakely, 1996). In general, $\vec{M}$ may change from point to point in direction and magnitude, and

ORIGINAL UNEDITED MANUSCRIPT

Downloaded from https://academic.oup.com/gji/advance-article/doi/10.1093/gji/ggad163/7120036 by Universidade do Porto user on 18 April 2023

may have both induced and remanent contributions. The observed frequency and amplitude content of the observed anomaly are thus strongly dependent on the observation distance and on the geometry and magnetisation of the causative bodies. In particular, the rate of amplitude decrease with the distance between the sensor and causative body depends on the body geometry and is usually expressed by the structural index or attenuation rate. In geological applications, anomalies are mainly caused by changes in the magnetisation distribution due to topographic variation of magnetised layers, edge effects at the borders of contrasting lithological units, and presence of singular magnetised bodies.

Here we evaluate the possible contribution of these types of magnetic sources for the magnetic anomaly observed along IAM-9. The effect of topography of the magnetised basement of the Iberia Abyssal Plain was extensively evaluated by Russell and Whitmarsh (2003) by analysis of the magnetic anomaly measured by sea-level and deep-tow shipborne magnetic data.

2.1. Cross-section forward modeling

We use magnetic forward modeling to reproduce previous models and to propose a new geological model along IAM-9. The magnetic response of geological models was calculated using the GMSYS modelling package of *Oasis montaj* (Geosoft), which calculates the magnetic response of a multiple-bodies domain based on the method of Talwani & Heirtzler (1964). We considered the geographical location (Figure 1) and trending (9°W) of IAM-9 profile, and an IGRF-determined inducing field (at the time of survey) of 44 150 nT ; Inc = 55.4° ; Dec = -7.4°.

ORIGINAL UNEDITED MANUSCRIPT

Downloaded from https://academic.oup.com/gji/advance-article/doi/10.1093/gji/ggad163/7120036 by Universidade do Porto user on 18 April 2023

For reproducing Bronner et al. (2011) and Russell and Whitmarsh (2003) models, we digitised the original geometry of the layers and compared the calculated anomaly to the observed magnetic data respectively presented in those works. We assigned to each layer the original magnetic parameters, including the remanent magnetization parameters for magmatic layers: Inc=46°; Dec=0° as used by both studies. The parameters of our new magnetic model are described in Section 4.

2.2.Synthetic models

To evaluate the expected contributions of edge effects and magnetised bodies at different depths, with different geometry and magnetic parameters, we produced several sets of synthetic models. Synthetic tests were produced using the MAGPRISM software (https://sites.google.com/view/markkussoftware/gravity-and-magnetic-software) that computes the magnetic field above a magnetised prism-like body based on the algorithm of S.-E. Hjelt (1972). Graphical representation was made using the Python *matplotlib* library.

Synthetic models were computed as W-E striking profiles. This simplification with respect to the real 9°W strike of the IAM-9 allows to focus the interpretation on the tested parameters. In Supplementary Text A and Supplementary Figure S1 we tested the effect of the 9° change of profile strike, showing that it has a negligible effect.

Synthetic models use an inducing field of 44 150 nT; Inc=55.4°; Dec=0°. Although the local IGRF field has non-zero declination, this simplification also allows to focus on the parameters being tested in each synthetic model. Supplementary Text B and Supplementary Figure S2 test the effect of using inducing field declination values of 0°, -4° or -8°, showing that the

ORIGINAL UNEDITED MANUSCRIPT

Downloaded from https://academic.oup.com/gji/advance-article/doi/10.1093/gji/ggad163/7120036 by Universidade do Porto user on 18 April 2023

amplitude and general shape of the anomaly are mostly maintained, with a change in symmetry that does not affect the interpretation.

3. PREVIOUS MAGNETIC MODELS OF IBERIA ABYSSAL PLAIN

In this section we reassess previous magnetic models of the structure of the Iberia Abyssal Plain, discuss potential technical and interpretative limitations, and present synthetic models that support our arguments and the discussion of using magnetic data to infer subsurface structures.

3.1. IAM-9 model 2011 (Bronner et al., 2011)

Bronner et al. (2011) forward modeled the seismic velocity structure along profiles of the WIM and conjugate Newfoundland margin with sea-level magnetic measurements. We reproduced their IAM-9 magnetic model, digitizing their layer structure and assigning the same magnetic parameters to calculate the magnetic anomaly response (Figure 2) (c.f. Section 2.1). Their model shows lava flows in the uppermost basement layer, and gabbro intrusions ~13-14 km deep in the basement.

ORIGINAL UNEDITED MANUSCRIPT

Downloaded from https://academic.oup.com/gji/advance-article/doi/10.1093/gji/ggad163/7120036 by Universidade do Porto user on 18 April 2023

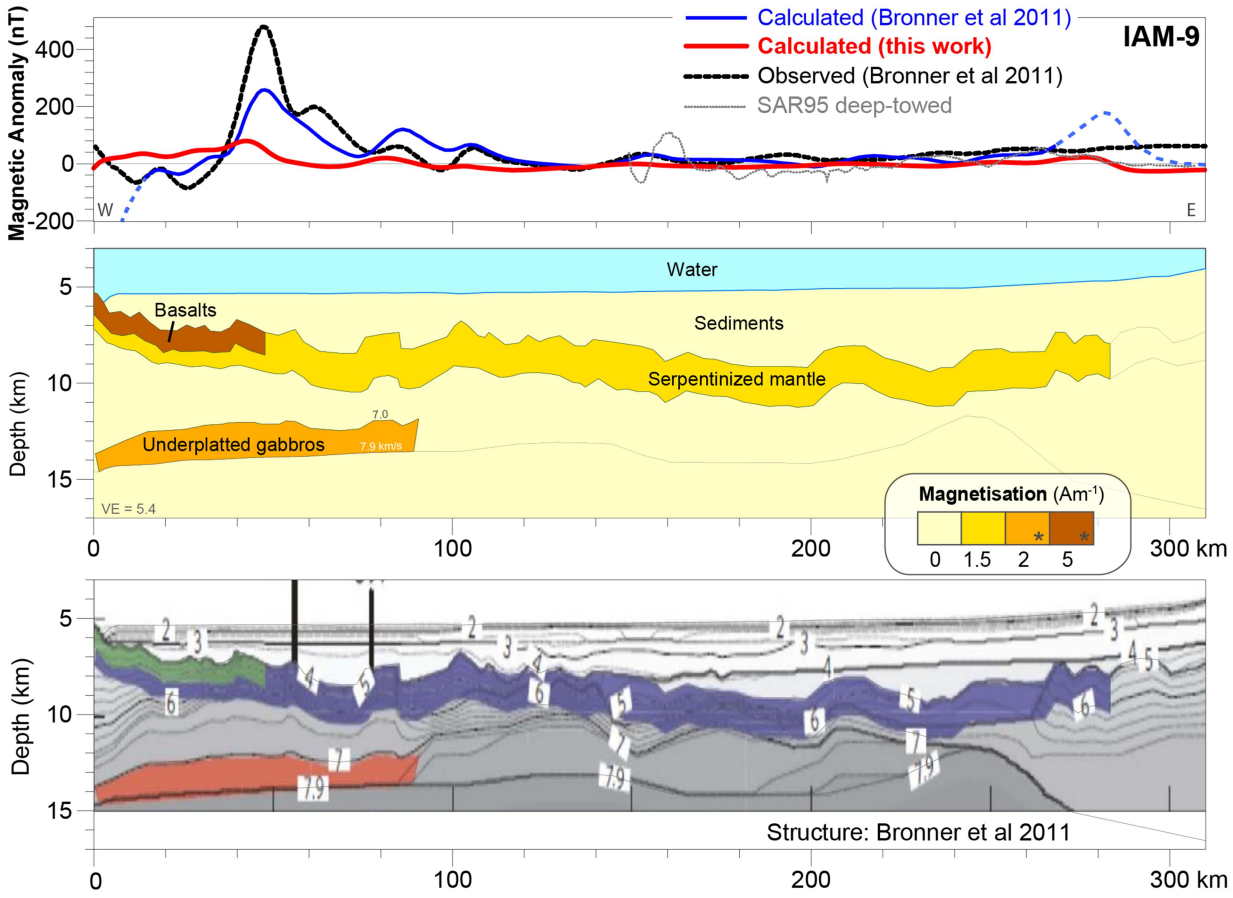

Figure 2. *Reproduction of crustal model and magnetic modelling by Bronner et al. (2011) along the IAM-9 profile. The magnetic response calculated in this work (red) is markedly different from the results of Bronner et al. (2011) (blue) in both amplitude and shape of anomalies, questioning their results. For model reproduction, we used the same geometry and the magnetic parameters given in Bronner et al. (2011), including the magnetic remanence used for basalt and gabbro layers (* in legend; c.f. Section 2.1). The calculated anomaly is compared to the observed magnetic data of Bronner et al. (2011).*

ORIGINAL UNEDITED

Downloaded from https://academic.oup.com/gji/advance-article/doi/10.1093/gji/ggad163/7120036 by Universidade do Porto user on 18 April 2023

The comparison shows up to ~200 nT difference between our test and the published calculated anomalies (red and blue lines in Figure 2). Bronner et al. (2011) show a calculated amplitude of ~250 nT for J-anomaly (blue line), resembling the shape, but with >200 nT of misfit with the shipborne data (black line). In contrast, our calculated response (red line) for the same structure yields anomalies of <100 nT amplitude and cannot explain the observed shipborne data. This numerical disparity for the same geological model and magnetic parameters led us to further evaluate these modelling results, testing the edge effects caused by equivalent magnetic layers.

3.1.1. Synthetic tests of sub-horizontal layers

Bronner et al. (2011) model (Figure 2) shows (i) the largest anomaly of ~250 nT caused by magnetisation contrasts (edge effect) over the edge of a basaltic layer at ~7-8 km depth covering low-magnetisation serpentinized mantle; (ii) a ~120 nT anomaly produced above the edge of a gabbro layer at ~12-14 km depth, underplating non-magnetised mantle.

To calculate the edge effect produced by the lateral termination of equivalent magnetised layers we modeled a 2 km thick tabular body at various depths (distance from the sensor), from 100 m to 12 km (Figure 3). The modeled susceptibility values (χ) are equivalent to the magnetisation contrasts used by Bronner et al. (2011): 0.06 SI corresponds to the 2 Am^{-1} assigned to the inferred 12-km-deep gabbroic layer (Figure 3a); and 0.1 SI corresponds to the 3.5 Am^{-1} magnetisation contrast between the inferred basalt layer and underlaying serpentinized peridotites at ~8 km depth (Figure 3b). The modeled prisms extend to the west

ORIGINAL UNEDITED MANUSCRIPT

Downloaded from https://academic.oup.com/gji/advance-article/doi/10.1093/gji/ggad163/7120036 by Universidade do Porto user on 18 April 2023

and along the N-S direction. Our simulations consider horizontal layers, comparable with Bronner et al. (2011) layers of ~1° dip.

These synthetic magnetic tests show that the edge effect of the two equivalent layers produce anomalies of much smaller amplitude than the anomalies presented by Bronner et al. (2011). The modeled amplitudes (peak-to-trough) are <40 nT for the 12 km depth gabbro layer (Figure 3a) and <130 nT and 100 nT for the 6 km and 8 km depth basaltic layers, respectively (Figure 3b). These values are 2 to 3 times smaller than the Bronner et al. (zero-to-peak) calculated anomalies (~120 nT and ~250 nT), and much smaller than the ~450 nT maximum measured anomaly (Figure 2). Furthermore, this test shows that to measure anomalies with amplitudes ~120 - 250 nT as those caused by the basement structure in Bronner et al. (2011), a magnetometer would need to be towed 2 – 0.5 km, respectively, above the 2-km-thick causative layer edge. This is clearly impossible for IAM-9 as the basement is covered by several km of sediment along most of the line, and only at the western end the basement shallows towards the seafloor, when approaching a volcanic seamount (Figure 1; Figure 2).

The additional test in Supplementary Text C and Supplementary Figure S3 shows the effect on the anomaly amplitude of changes in thickness of a magnetized layer using 7 km for the top-of-the-layer depth, similar to the basement depth in the Iberia Abyssal Plain. The test shows, at this depth, the layer thickness has a measurable contribution, resulting from the volume integration in Equation 1.

ORIGINAL UNEDITED MANUSCRIPT

Downloaded from https://academic.oup.com/gji/advance-article/doi/10.1093/gji/ggad163/7120036 by Universidade do Porto user on 18 April 2023

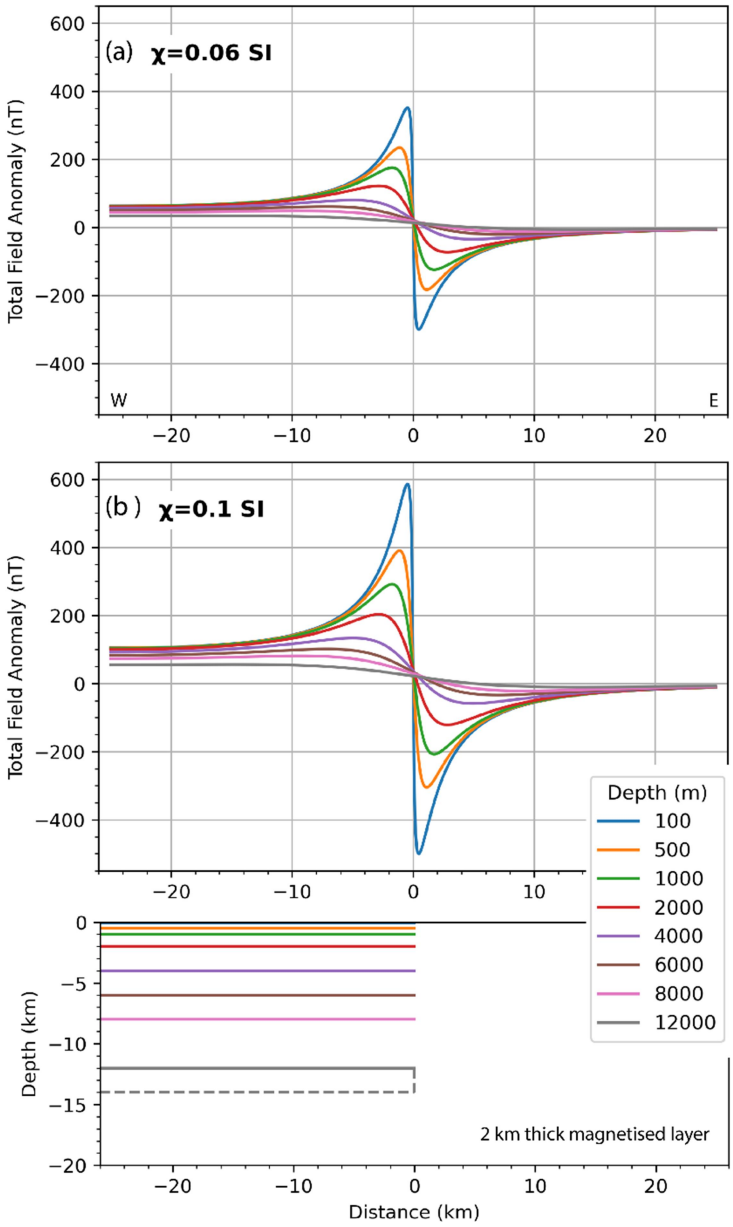

Figure 3. *Synthetic magnetic models - 1. Edge-effect magnetic anomaly caused by the lateral termination of a 2 km-thick 3D tabular magnetised body placed at depths from 100 m to 12 km. We consider two susceptibility values for the magnetised layer, corresponding to equivalent magnetisation contrasts in Bronner et al. (2011) model:* ***(a)*** *χ=0.06 SI corresponds to the gabbro layer with 2 Am^{-1} magnetisation; and* ***(b)*** *0.1 SI corresponds to the 3.5 Am^{-1}*

ORIGINAL UNMANUSCRIPT

Downloaded from https://academic.oup.com/gji/advance-article/doi/10.1093/gji/ggad163/7120036 by Universidade do Porto user on 18 April 2023

magnetisation contrast between the basalt layer and underlaying serpentinized peridotites. The edge-effect amplitude decreases rapidly with depth. For a 7-8 km-deep basaltic layer (a) or a 12 km-deep underplated gabbro (b), the response anomaly (<120 nT and <40 nT, respectively) is negligible when compared to the observed J-anomaly amplitude of 350-450 nT. In the bottom panel is represented the location of the modeled layers. For simplicity, only the deeper layer shows the total 2 km thickness (dashed gray line), while for the other layers only the top is represented.

3.2. The effect of the top of basement relief

The low amplitude anomalies (~40 nT) measured at sea level in the eastern half of IAM-9 are associated to the effect caused by lateral variations of the relief of the top of the basement in the model of Bronner et al. (2011) (Figure 2). In contrast, Russell and Whitmarsh (2003) analysis of deep-tow data profiles in the Iberia Abyssal Plain indicates that basement relief alone cannot explain these anomalies, which must instead be due to magnetization contrasts within the crust. Sibuet et al. (2007) reassessed Russel and Whitmarsh's analysis agreeing with this conclusion, although they question the source depth estimation method and claim that Russell and Whitmarsh Euler deconvolution may be biased by the necessary assumptions of structural indices. Sibuet et al. (2007) support source depths within the upper 3 km of the basement, which is shallower than the 6-8 km below the top of the basement estimations of Russell and Whitmarsh (2003).

ORIGINAL UNEDITED MANUSCRIPT

Downloaded from https://academic.oup.com/gji/advance-article/doi/10.1093/gji/ggad163/7120036 by Universidade do Porto user on 18 April 2023

The model results from Russell and Whitmarsh (2003) and Sibuet et al. (2007) are in line with our calculations in Figure 2 (red line, forward anomaly calculated at sea-level), which show that the basement relief measured along seismic IAM-9 and located at 7-9 km depth below sea level, is mostly undetectable by measurements with magnetic sensors towed at sea level.

Therefore, synthetic tests and model replication demonstrate that (1) the magnetic sources in the structure of Bronner et al. (2011) model cannot be constrained by magnetic data measured at sea-level; (2) the anomaly response obtained by Bronner et al. (2011) is numerically incorrect, implying methodological problems. Since the same modelling method was applied by the same authors to other transects of the West Iberia and of the conjugate Newfoundland margins, it is reasonable to argue that those magnetic models and the geological cross-sections inferred by Bronner et al. (2011), both from the WIM and conjugate Newfoundland, are unconstrained and the model results physically improbable.

3.3. IAM-9 model 2020 (Szameitat et al., 2020)

A study reassessing Bronner et al. (2011) along IAM-9 (Szameitat et al., 2020) used a different software (GMsys software), which we also use in this work. Their IAM-9 model presents a slightly modified geometry of the layers that produces a different magnetic anomaly response. Particularly, the upper (basaltic) layer in their model is not a subhorizontal and constant thickness layer, as in Bronner et al. (2011), but has variable thickness, including a thicker ~20 km wide central segment. This thicker central segment seems to be the causative source of a ~140 nT magnetic anomaly maximum amplitude, which is about 2-3 times smaller than the observed J-anomaly amplitude. Moreover, even despite the more favorable body geometry,

ORIGINAL UNEDITED MANUSCRIPT

Downloaded from https://academic.oup.com/gji/advance-article/doi/10.1093/gji/ggad163/7120036 by Universidade do Porto user on 18 April 2023

the maximum amplitude retrieved by Szameitat et al. (2020) achieves only 50-60% of the ~250 nT amplitude shown by Bronner et al. (2011), which further supports that the anomaly calculation by Bronner et al. (2011) is incorrect.

3.4. LG-12 model 2016 (Stanton et al., 2016)

Stanton et al. (2016) modeled the J-anomaly as produced by two magnetized igneous layers (basalt and oceanic gabbros), separated by a thin layer of serpentinised mantle. They model the northern edge of the large amplitude J-anomaly along the seismic line Lusigal-12 (LG12) ~25 km north of IAM-9 (Figure 1). Their proposed geometry is a 3-4 km thick basalt layer overlaying a 3-4 km gabbro, but it is unconstrained by seismic (or any other) data and is unknown as a geological structure in the region, i.e. it is neither oceanic crust structure nor exhumed and intruded mantle. They describe that the regular magnetization values they use are insufficient to produce anomalies of amplitude similar to the J-anomaly, and their modelled anomaly is about half of the observed anomaly. Thus, Stanton et al. (2016) results further support that to reach the observed amplitude an increased magnetization is needed.

3.5. IAM-9 model 2003 (Russell and Whitmarsh, 2003)

The first magnetic forward modelling along IAM-9 was done by Russell and Whitmarsh (2003) following the interpretation of the seismic velocity model of Dean et al. (2000), and led to propose the J-anomaly as a seafloor spreading lineation, as well as the existence of oceanic crust extending ~40 km further east. Russell and Whitmarsh (2003) modeled basement-thick magnetised blocks with alternating polarities (isochrons with $\pm 0.8\ Am^{-1}$), using basement

ORIGINAL UNEDITED MANUSCRIPT

Downloaded from https://academic.oup.com/gji/advance-article/doi/10.1093/gji/ggad163/7120036 by Universidade do Porto user on 18 April 2023

thickness, overall structure, and the top of the basement topography from Dean et al. (2000) model.

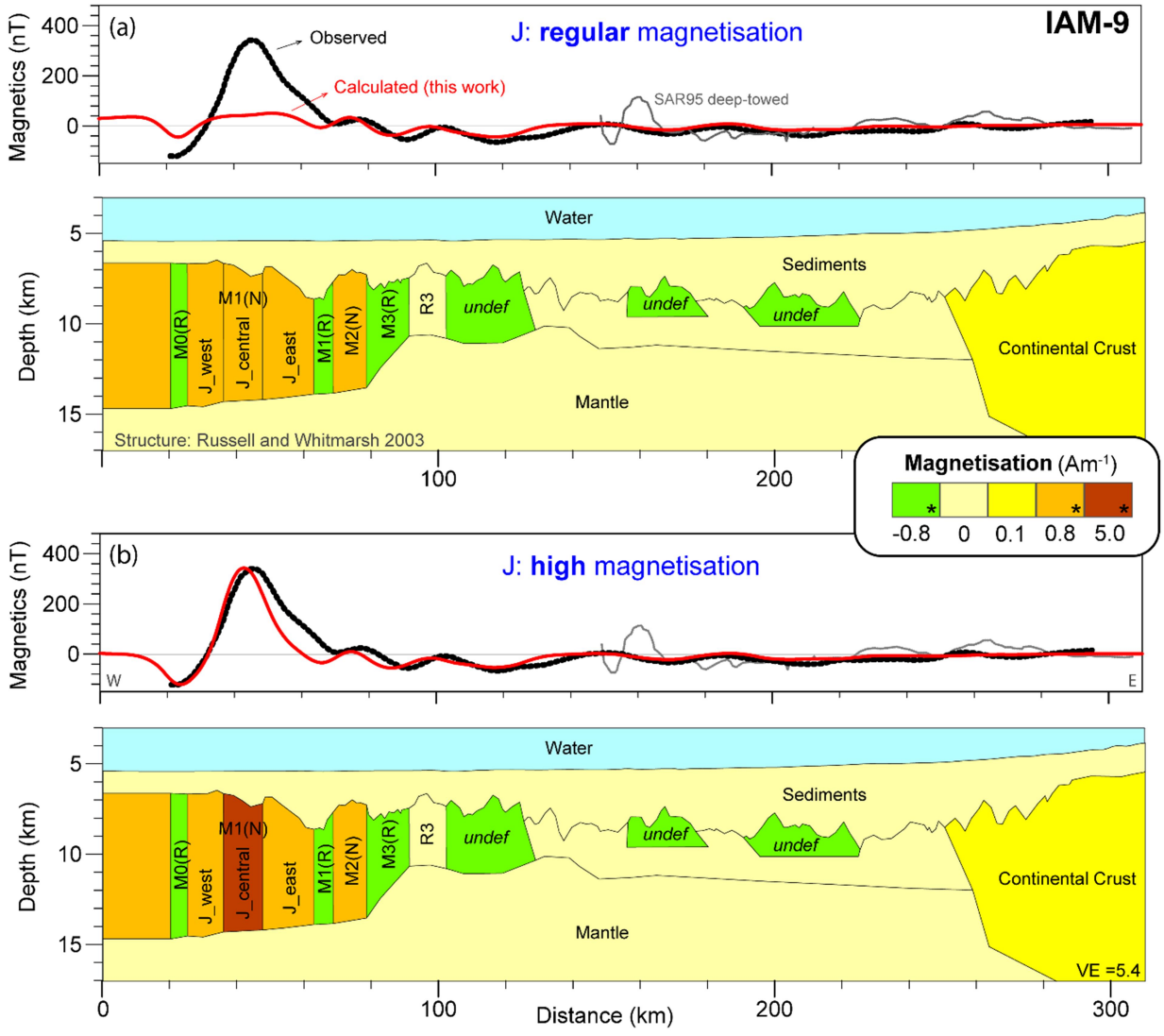

Figure 4. *Reproduction of Russell and Whitmarsh (2003) magnetic model along line IAM-9. Blocks west of km 100 were interpreted as seafloor spreading blocks with ±0.8 Am^{-1} magnetisation (isochrons); blocks labeled "undef" are undefined-age magnetic bodies, assumed to be magmatic bodies with negative remanence; R3 is a non-magnetic block. Magnetisation labeled with * indicates magnetic remanence; c.f. Section 2.1.* ***(a)*** *J-anomaly is*

ORIGINAL U

Downloaded from https://academic.oup.com/gji/advance-article/doi/10.1093/gji/ggad163/7120036 by Universidade do Porto user on 18 April 2023

modeled with constant magnetisation (0.8 Am^{-1}) in the three blocks defined by Russell and Whitmarsh (2003). ***(b)*** *The J-anomaly central block is assigned a higher magnetisation (~6 times larger than J-east and J-west blocks), in agreement with our synthetic tests in Figure 5. The results show that the magnetic amplitude corresponding to the J-anomaly is only achieved - for this basement geometry - when one block has higher magnetisation. Observed magnetic anomaly data is shipborne data, from Russelll & Whitmarsh (2003).*

Following with the tests, we also reproduced Russell and Whitmarsh (2003) magnetic model (Figure 5). Figure 5a reproduces the model with oceanic blocks assigned ±0.8 Am^{-1} magnetisation with alternating polarities, as originally described. As can be noted, however, this constant ±0.8 Am^{-1} magnetisation is not sufficient to explain the measured ~350 nT amplitude of the J-anomaly (Figure 5a). As we show in Figure 5b, to match the J-anomaly amplitude a local 6-fold increase in magnetisation (to 5 Am^{-1}) is required for the central crustal block, which corresponds to the J-anomaly. Although not discussed neither in the main text nor in the caption of figure 12 of Russell and Whitmarsh (2003), nor by Sibuet et al. (2007) who reanalysed their results, it is likely that Russell and Whitmarsh (2003) recognised the need for this increase in magnetisation since they present an inverse derived magnetisation solution (bottom panel of their figure 12) with about 5 Am^{-1} calculated for the J-anomaly block, matching our inference of locally-increased magnetisation. This set of observations further support our conclusion that edge contrasts due to a relatively thin magnetic layer

ORIGINAL UNEDITED MANUSCRIPT

Downloaded from https://academic.oup.com/gji/advance-article/doi/10.1093/gji/ggad163/7120036 by Universidade do Porto user on 18 April 2023

cannot explain the comparatively large J-anomaly magnetic amplitude (unless unlikely large magnetisation contrast is considered), as shown by the synthetic model results (Figure 3).

3.5.1. Synthetic tests of a uniformly magnetised body

To independently test the need for an increased magnetisation block, we produced a second set of synthetic tests on the effect of changing the magnetisation of a body with dimensions and depths similar to the blocks causing the J-anomaly (Figure 5). We modeled a magnetised block that simulates the thickness of the igneous crust of the basement along IAM9 (15 km wide and extending from 7 to 14 km depth), with magnetisation values varying from 0.3 to 10 Am^{-1}. These tests show that an anomaly amplitude of ~400 nT, comparable to the J-anomaly measured at sea-level, will be caused by a body with magnetisation >5 Am^{-1} ($\chi > 0.15$ SI), for this body geometry. This further supports that the J-anomaly may be caused by a basement body with high magnetisation, similar to the modelling of Russell and Whitmarsh (2003) (Figure 4).

In Supplementary Text D and Supplementary Figure S4 we present additional tests on the effect of changing the width of the magnetised body. For widths >30 km the anomaly shows the superposition effect of two edge anomalies from each side of the body, while for widths <30 km a single long-wavelength anomaly is observed, with amplitude rapidly decreasing with decreasing width.

ORIGINAL UNEDITED MANUSCRIPT

Downloaded from https://academic.oup.com/gji/advance-article/doi/10.1093/gji/ggad163/7120036 by Universidade do Porto user on 18 April 2023

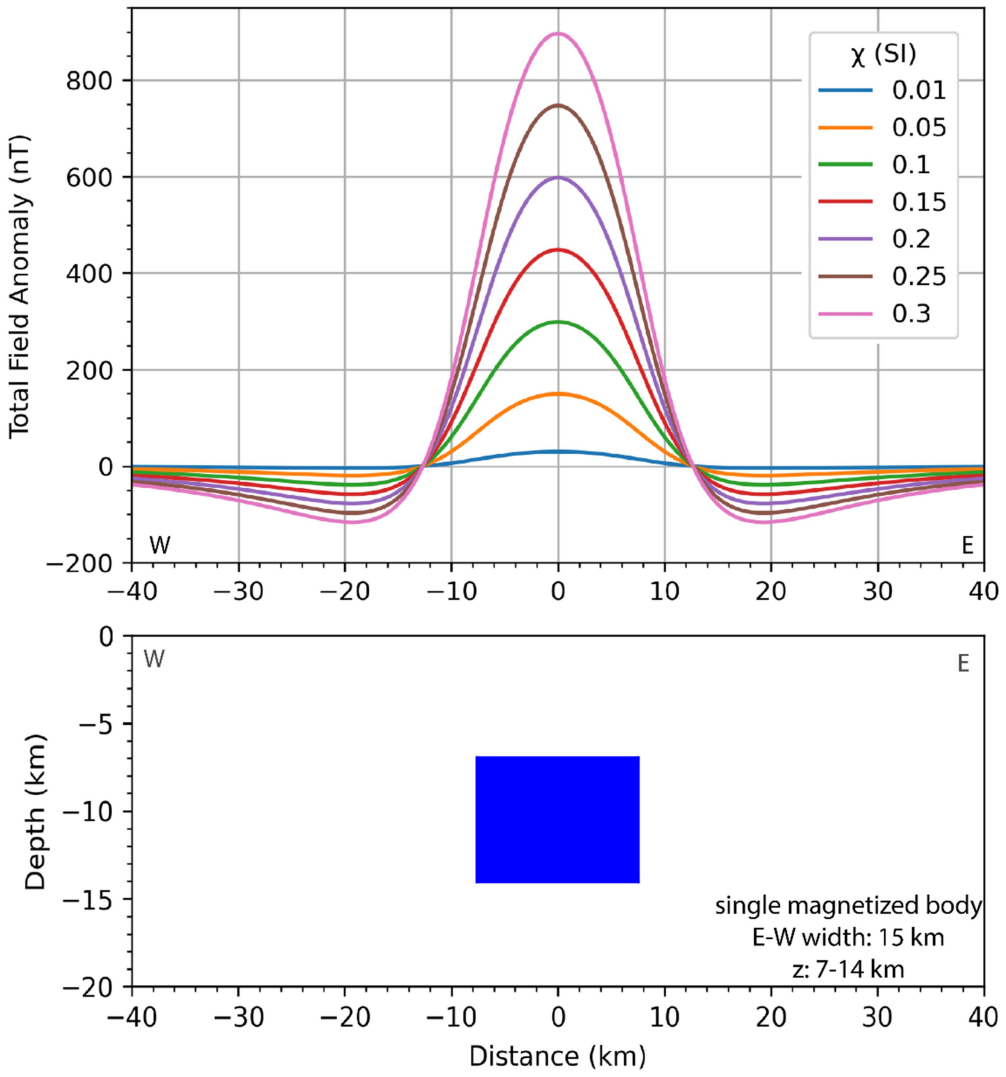

Figure 5. *Synthetic magnetic models - 2. Magnetic anomaly caused by a single-magnetised body with susceptibility ranging from 0.01 SI to 0.3 SI (equivalent 0.3 - 10 Am^{-1} magnetisation range). The body depth and dimensions are comparable to a basement-thick J-central block as modeled by Russell and Whitmarsh (2003) (Figure 4). Magnetic anomaly values comparable to the J-anomaly amplitude are reached for χ = 0.15 SI (≈ 5 Am^{-1} magnetisation).*

ORIGINAL UNEDITED MANUSCRIPT

Downloaded from https://academic.oup.com/gji/advance-article/doi/10.1093/gji/ggad163/7120036 by Universidade do Porto user on 18 April 2023

In summary, there is no physical support for the edge effect of sub-horizontal magnetic layers to be the causative structure producing the measured magnetic anomalies as originally proposed by Bronner et al. (2011). Our analysis supports that the J-anomaly is likely caused by a crustal block with increased magnetisation.

3.6. Seismic constraints and uncertainties

Additional constraints on the geometry of the magnetisation distribution, as well as on the nature of the magnetic sources, may be given by independent geophysical data informing on the crustal structure, e.g., seismic velocity structure. The wide-angle seismic velocity model of Dean et al. (2000) was invoked to justify some aspects of the geological structure in Russell and Whitmarsh (2003) and Bronner et al. (2011) models. However, we discuss here how the intrinsic uncertainty integral to the estimation of seismic velocity (Vp) models was underappreciated, and the constraints provided by that Vp model on physical properties are over-interpreted in some cases.

The uncertainty inherent to IAM-9 wide-angle seismic data and modelling approaches is clearly illustrated by the differences between Vp models obtained using the same field data set and similar forward modelling approaches, using the OBS arrival travel time picks. This is illustrated in Figure 6. The differences in Vp distribution among the models from Dean et al. (2000) (Figure 6a) and Minshull et al. (2014) (Figure 6b) support a minimum ~20 km offset of their respective boundary between exhumed mantle and oceanic crust, and perhaps as much as 30 km (Minshull et al., 2014). Furthermore, a new Vp model calculated using the same

ORIGINAL UNEDITED MANUSCRIPT

Downloaded from https://academic.oup.com/gji/advance-article/doi/10.1093/gji/ggad163/7120036 by Universidade do Porto user on 18 April 2023

travel-time picks of Minshull et al. (2014) but with a tomographic (inversion) approach (Grevemeyer et al., 2022) changes further the Vp distribution and the contact between exhumed mantle and oceanic crust structure (Figure 6c). The tomographic Vp model supports to change the boundary further west by another ~25 km, i.e., as much as ~45 km west of Dean et al. (2000) interpretation. The interpretation of the contact between exhumed mantle and oceanic crust next to the J-anomaly basement is further strengthened by the estimation of velocity uncertainty, which is reasonably low to support the results of the tomographic approach (Grevemeyer et al., 2022). The forward modelling approaches provide limited, fundamentally qualitative, information on model uncertainty.

The variable location of the exhumed mantle – oceanic crust boundary in the three models is caused by the limited resolution imposed by the comparatively scarce ray coverage in the COT basement in the transition between the J-anomaly and exhumed mantle, due to the OBSs separation of ~60 km there (Figure 1; Figure 6). In addition to this limitation in data resolution, an additional limitation may arise from the subjectivity involved in forward modelling approaches, when compared to the somewhat more objective tomographic inversion method.

Irrespective of the quality of the travel time picks and methodological approach, travel time modelling with OBS that are separated several tens to ~60 km, like along IAM-9, do not allow to determine the dimensions of the basaltic and intrusive gabbro layers, let alone define their geometry in relation to the serpentined mantle, as proposed by Bronner et al. (2011). Even the new wide-angle seismic data at the WIM with ~10 km OBS spacing could not resolve similar structures, as indicated by uncertainty analysis and resolution tests (Merino et al., 2021a; Grevemeyer et al, 2022).

ORIGINAL UNEDITED MANUSCRIPT

Downloaded from https://academic.oup.com/gji/advance-article/doi/10.1093/gji/ggad163/7120036 by Universidade do Porto user on 18 April 2023

Finally, Bronner et al. (2011) attribute the high amplitude and steep western flank of J-anomaly to a volcanic seamount at the western end of IAM-9. However, this justification is insufficient, as it does not explain the linear character of J-anomaly running along the entire Iberia Abyssal Plain, and although offset, running also along the Tagus Abyssal Plain (Figure 1).

The presented arguments support that, besides the unresolved methodological issues on the magnetic modelling approach of Bronner et al. (2011) (cf. previous sections), their geological model also suffers from over-interpretation of seismic velocity data, and the detailed geological structures proposed for the WIM cross-sections, beyond the resolution of available seismic data, is unsupported.

ORIGINAL UNEDITED MANUSCRIPT

Downloaded from https://academic.oup.com/gji/advance-article/doi/10.1093/gji/ggad163/7120036 by Universidade do Porto user on 18 April 2023

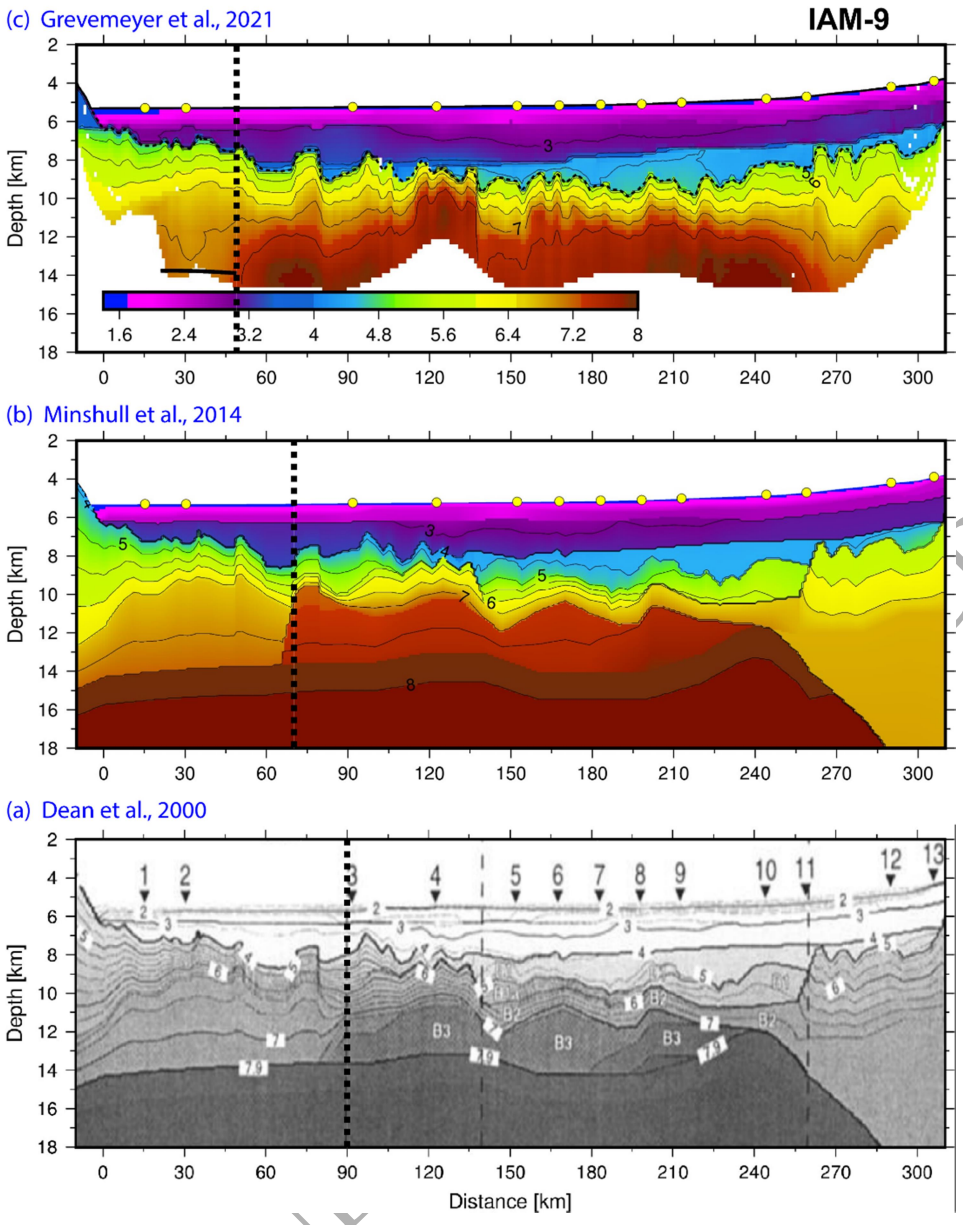

Figure 6. *P-wave velocity (Vp) models of the IAM-9 wide-angle seismic line. The three models are built from travel-time picks of the same 13 Ocean Bottom Seismometer records. The dashed vertical line marks the interpreted boundary between exhumed mantle and oceanic crust for each model, taken from the original publications.* ***(a)*** *Vp model obtained from forward modelling by Dean et al., (2000).* ***(b)*** *Revised forward model by Minshull et al. (2014). The boundary between exhumed mantle and oceanic crust is moved 20 km westwards with respect*

ORIGINAL UNPUBLISHED MANUSCRIPT

Downloaded from https://academic.oup.com/gji/advance-article/doi/10.1093/gji/ggad163/7120036 by Universidade do Porto user on 18 April 2023

to Dean et al. (2000). ***(c)*** *Travel time tomographic model obtained by Grevemeyer et al. (2022) with the travel time picks of Minshull et al., 2014. The boundary between exhumed mantle and oceanic crust is further displaced 25 km to the west, at the edge of the J-anomaly basement. The significant changes in location of the boundary are caused by the uncertainty in Vp determination arising from the large distance between OBS 2 and 3, which are >60 km apart, resulting in low ray coverage on the upper ~8 km of the crystalline basement.*

4. NEW GEOLOGICAL MODEL

4.1. Building a new IAM-9 magnetic model

4.1.1. Seismic constraints for the definition of magnetic layers

We use the structure of the seismic velocity model obtained with travel time tomography (Grevemeyer et al., 2022; Figure 6c) to build a new magnetic model for the IAM-9 profile, presented in Figure 7. The tomographic model produces results for the distribution of continental crust and most of the exhumed mantle domain similar to previous forward velocity models (Dean et al., 2000; Minshull et al., 2014), but the contact with the oceanic crust is different. Further, the tomographic model includes uncertainty estimation (Grevemeyer et al., 2022), providing improved information on the reliability of Vp constraining geological features.

To build our model, we have not added any extra rock body unconstrained by the seismic model; thus, we have not attempted to increase the resolution of the seismic results using

ORIGINAL UNEDITED MANUSCRIPT

Downloaded from https://academic.oup.com/gji/advance-article/doi/10.1093/gji/ggad163/7120036 by Universidade do Porto user on 18 April 2023

sea-level magnetic data, which in this deep-water context is unfeasible as demonstrated by the synthetic tests (Figure 3).

We integrated the seismic boundaries between continental crust, exhumed mantle, and oceanic crust domains. In the continental domain, the limit between upper and lower crystalline basement was defined at the 6.5 km s^{-1} iso-velocity. Oceanic crust was assigned a layer 2/3 structure with the transition at the 6 km s^{-1} iso-velocity, and is bounded at depth by the Moho.

From the seismic structure point of view, the Layer 2/3 boundary for old oceanic crust is 6.5 km/s (e.g. Christeson et al., 2019). However, we use 6.0 km/s to define the base of the basaltic crust with comparatively higher magnetisation than the lower crust. This is because from 6.0 to 6.5 we expect sheeted dikes with a magnetic signature similar to gabbro. However, we have tested the alternative model with 6.5 km/s as layer 2/3 limit (Supplementary Text E and Supplementary Figure S5), showing that even considering this thicker layer 2, a high magnetisation is needed, compared to regular oceanic crust, to fit the observed anomaly.

The Vp of the western edge of the profile is ill-defined at depth due to low ray coverage and the added complexity of a nearby volcanic edifice clearly visible in the bathymetry (Figure 1), and thus the Moho depth for this edge sector was maintained with respect to J-anomaly basement. However, in case of a thinner crust in the sector, it would not change the conclusion that J-anomaly basement requires a higher magnetisation.

ORIGINAL UNEDITED MANUSCRIPT

Downloaded from https://academic.oup.com/gji/advance-article/doi/10.1093/gji/ggad163/7120036 by Universidade do Porto user on 18 April 2023

4.1.2. Magnetic parameters

Magnetic parameters for oceanic crust were assigned according to Gee and Kent (2007) and references therein, and remanent magnetisation was assumed with remanence parameters taken from the Iberian apparent polar wander path of Neres et al. (2012) for Lower-Upper Cretaceous ages (Inc = 48° and Dec = -15°). In the J-anomaly segment, increased magnetisation was necessary to fit the observed anomaly.

In the exhumed mantle domain, we considered as magnetic source only the top portion with estimated serpentinization degree larger than 60% (based on Vp; Sallarès et al 2011) which is the minimum degree needed to produce enough magnetite content for significant induced magnetisation (Oufi et al., 2002; Maffione et al., 2014). Continental and exhumed mantle domains are assigned induced magnetisation.

As observed magnetic anomaly, we consider along-profile data extracted from the regional compilation grid of Verhoef et al. (1996), which is similar to the observed magnetic data of Russell and Whitmarsh (2003) (Figure 4).

ORIGINAL UNEDITED MANUSCRIPT

Downloaded from https://academic.oup.com/gji/advance-article/doi/10.1093/gji/ggad163/7120036 by Universidade do Porto user on 18 April 2023

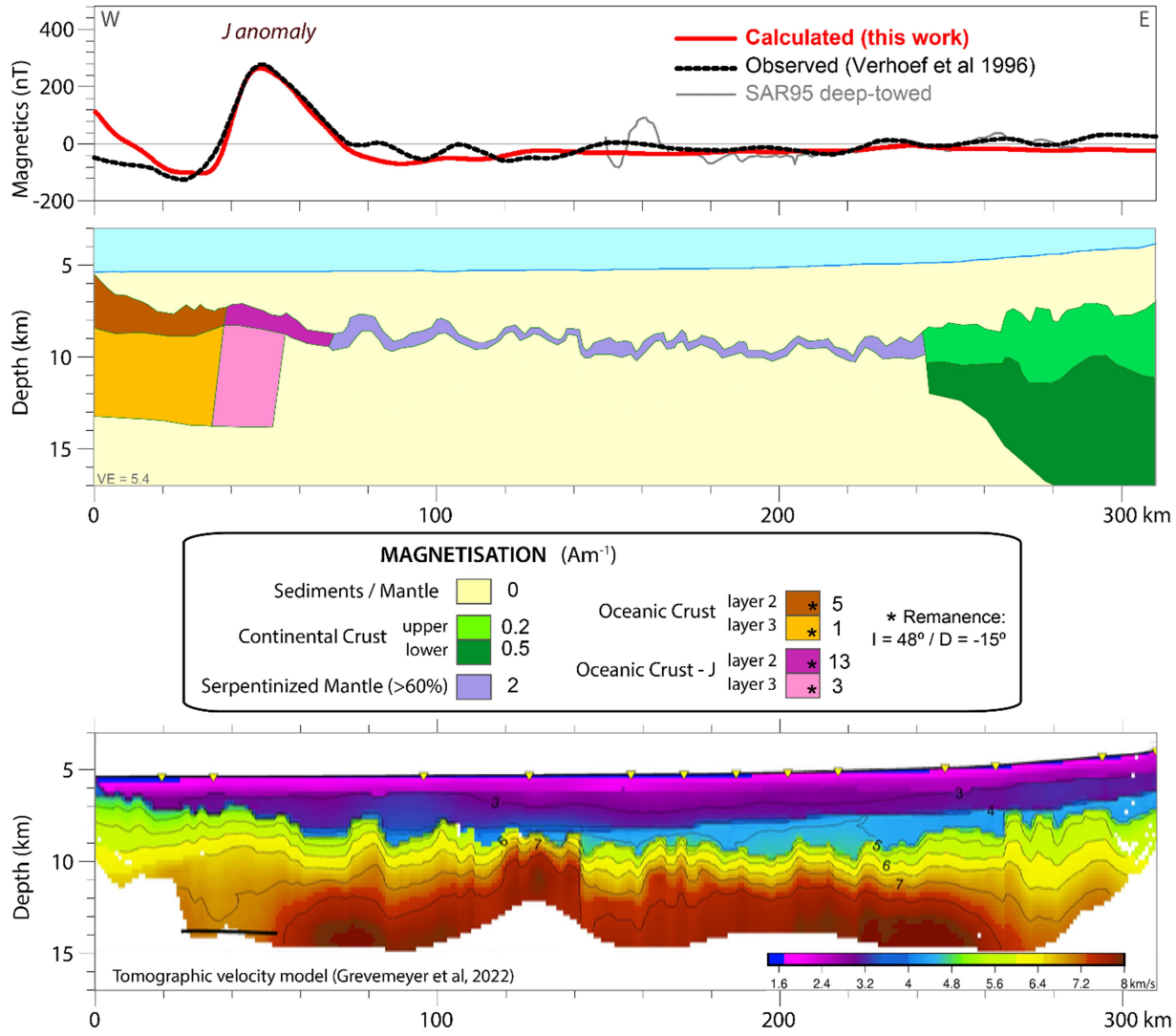

Figure 7. *New magnetic model for IAM-9, constrained by the seismic velocity structure of IAM-9 obtained by a travel time tomographic inversion model (Grevemeyer et al., 2022). Black line: Moho observed as wide-angle reflections. Magnetic sources: continental crust (upper/lower), oceanic crust (layer 2/3) and the top serpentinized mantle of the exhumed mantle domain, with inferred >60% degree of serpentinization. The observed J-anomaly amplitude requires, along ~20 km, values of magnetisation ~3 times higher than the westernmost regular oceanic crust. The J-anomaly crust marks the occurrence of the first oceanic crust, thus marking the COT boundary in abrupt contact with the eastern exhumed mantle domain.*

ORIGINAL UNEDITED

Downloaded from https://academic.oup.com/gji/advance-article/doi/10.1093/gji/ggad163/7120036 by Universidade do Porto user on 18 April 2023

4.2. New geological model

Our new magnetic model (Figure 7) has a simpler structure compared to previous models. The model fits well the J-anomaly amplitude and shape using a ~20 km-wide layer 2/3 oceanic crust structure, limited at depth by the wide-angle seismic Moho, and using an increased magnetisation (13 Am^{-1} and 3 Am^{-1} for layers 2 and 3, respectively) compared to normal oceanic crust to the west (5 Am^{-1} and 1 Am^{-1}) (Gee & Kent, 2007). Note that a thicker definition of layer 2 would not be enough to explain the anomaly, so that a comparatively high magnetisation appears unavoidable for the J-anomaly amplitude (c.f. Supplementary Text E; Supplementary Figure S5). A similarly simple magnetic source might be generalized to explain the linear J-anomaly along the Iberia and Tagus Abyssal Plain (Figure 1).

In this new magnetic model, the J-anomaly delimits the seaward extension of mantle-exhumation and therefore is the boundary of the COT. The magnetic inference for the first occurrence of oceanic crust, abutting the exhumed mantle domain, is consistent with the tomographic velocity models of Grevemeyer et al (2022). For completeness, we tested alternative definitions of the eastward limit of oceanic crust (e.g. Minshull et al., 2014), but the fit of the J-anomaly is comparatively less satisfactory (c.f. Supplementary Text F and Supplementary Figure S6).

Our model (Figure 7) has an asymmetric structure of the magnetic source that is able to produce the observed anomaly in amplitude, wavelength and slope. The boundaries of layer 3 are constrained by the Vp structure (Grevemeyer et al., 2022). But for the upper oceanic layer 2 (basaltic layer) an extension to the east helps explaining the eastern slope of the J-anomaly.

ORIGINAL UNEDITED MANUSCRIPT

Downloaded from https://academic.oup.com/gji/advance-article/doi/10.1093/gji/ggad163/7120036 by Universidade do Porto user on 18 April 2023

The integration of basaltic layers in the interpretation of the transition from exhumed mantle domain to oceanic crust appears supported by the seismic image of re-processed profile IAM-9 (Figure 8).

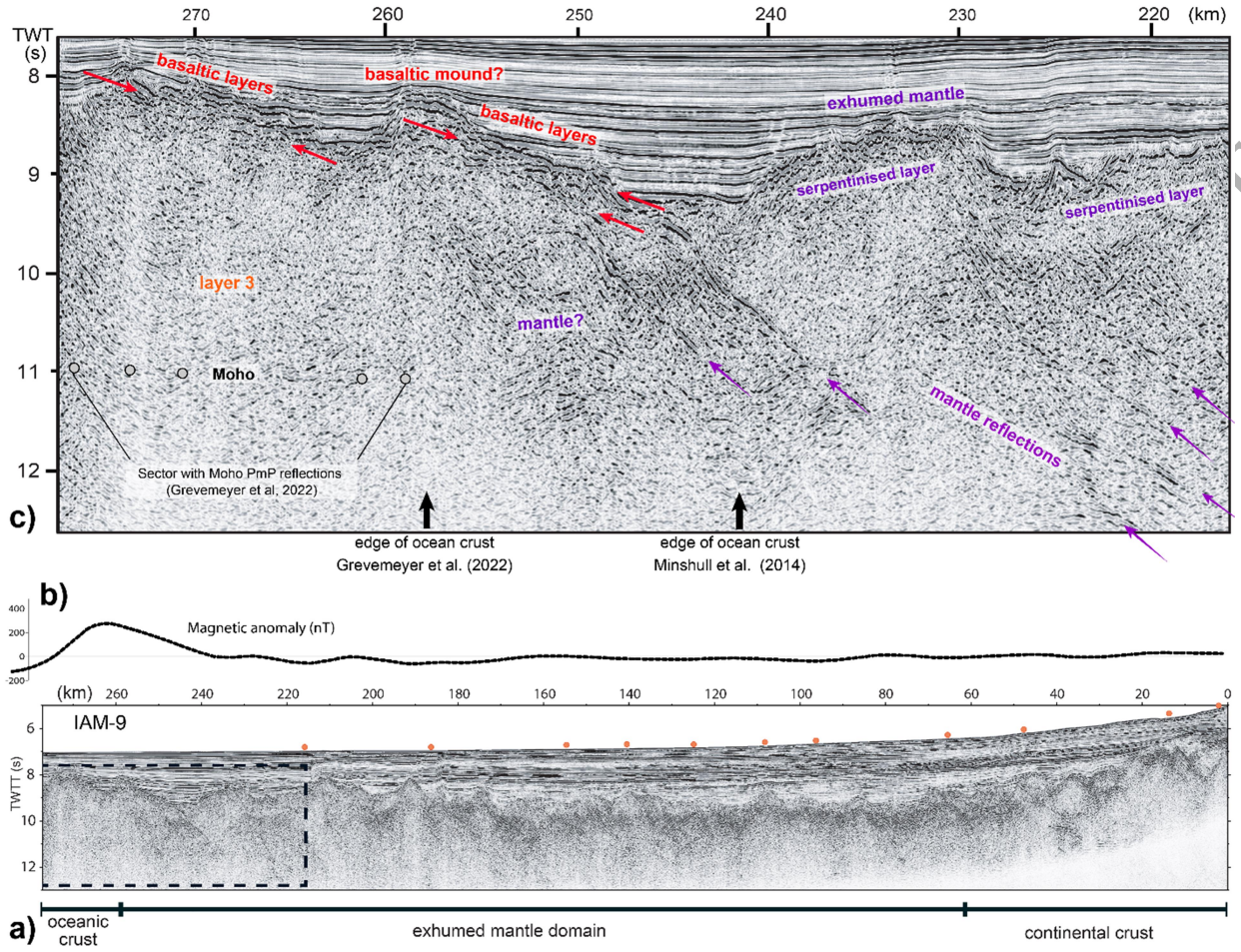

Figure 8: ***(a)*** *Reprocessed seismic reflection profile IAM9. The dashed-line box marks the segment of the close-up image shown in (c).* ***(b)*** *IAM-9 magnetic anomaly profile (Verhoef et al., 1996).* ***(c)*** *Close up of the transition from exhumed mantle to ocean crust. Interpretation integrates the information from wide-angle seismic models (Minshull et al., 2014; Grevemeyer et al. 2022).*

ORIGINAL UNE

Downloaded from https://academic.oup.com/gji/advance-article/doi/10.1093/gji/ggad163/7120036 by Universidade do Porto user on 18 April 2023

Figure 8a displays well the exhumed mantle domain, which is characterised by a complex basement relief, an upper basement layer ~0.5 s TWT thick with low reflectivity, an underlaying highly reflective ~1 s TWT thick band of poorly organised reflections, and comparatively bright deep landward-dipping reflections. The transition to oceanic crust to the west is complex, with landward-dipping mantle reflections and the complex basement reflectivity gradually disappearing. The top of basement relief becomes somewhat smoother to the west, with some ~10 km long linear east-dipping segments (Figure 8c). The westernmost ~20 km display indistinct sub-horizontal reflections at ~11 s TWT that may represent oceanic Moho, and that spatially agree with the location of PmP wide-angle reflection (Grevemeyer et al., 2022).

We interpreted the upper basement reflective layering as basaltic lava flows. The layering forms packages ~0.5 s TWT thick with a geometry that may be interpreted to indicate flow downslope to the east. The layering occurs in two main packages: the western package (km 262-273) may extend over a ~8 km thick igneous oceanic crust, and the eastern package (km 249-260) may extend over basement that likely represents exhumed mantle. This would imply a scenario where the creation of the J-anomaly oceanic crust formed an extrusive layer, possibly related to a basaltic mound (km ~256-260) that outpoured submarine lava flowing to the east (Figure 8c). These lava flows may have a magnetic signature similar to the J-anomaly and their extent helps explaining the symmetry of the magnetic anomaly. Some types of Seaward Dipping Reflectors (SDR) are lava layers deposited underwater that extend >20 km (Hopper et al., 2003).

ORIGINAL UNEDITED MANUSCRIPT

Downloaded from https://academic.oup.com/gji/advance-article/doi/10.1093/gji/ggad163/7120036 by Universidade do Porto user on 18 April 2023

At the western end of the profile, the presence of a younger seamount (Figure 1) affects the magnetic anomaly field but does not extend to interfere with the J-anomaly.

In the exhumed mantle domain, our results show that the anomalies associated to basement top relief are not enough to explain the observed low amplitude anomalies. To focus on the discussion of the effect of basement top relief (c.f. Section 3.2), we did not include magmatic intrusions or other magnetic sources in the exhumed mantle domain. The nature and source depth of these anomalies have been debated by Russell and Whitmarsh (2003) and Sibuet et al. (2007) and is beyond the scope of this work. However, it is likely that additional high-resolution data, e.g. grid-like deep-tow data, are necessary to map the anomalies extension and model them properly.

5. DISCUSSION

The structure of the COT and J-anomaly inferred with magnetic modelling has been often used to interpret rifting processes and the plate kinematics of the Iberia-Newfoundland conjugate margins (Sibuet et al., 2007; Bronner et al., 2011; Stanton et al., 2016; Nirrengarten et al. 2017, 2018; Szameitat et al., 2020), which are processes critical to understand other events like the opening of the Bay of Biscay and the formation of the Pyrenees (e.g. Sibuet at al 2004; Vissers and Meijer, 2012; Barnett-Moore et al., 2017). Moreover, the inferred COT structure of the WIM is used as a template to interpret magma-poor rifted systems elsewhere (e.g. reviews by Peron-Pinvidic et al., 2013; Haupert et al., 2016; Manatschal et al., 2021; Chenin et al., 2021).

ORIGINAL UNEDITED MANUSCRIPT

Downloaded from https://academic.oup.com/gji/advance-article/doi/10.1093/gji/ggad163/7120036 by Universidade do Porto user on 18 April 2023

However, our synthetic tests (Figure 3; Figure 4) show that sea-level magnetic data do not have the vertical resolution to provide the observations necessary to determine sub-horizontal layering within the COT basement, particularly at several km of water depth and under several km of sediment of a typical abyssal plain. Thus, as a general rule, magnetic modelling of the COT cannot increase the layer resolution obtained with seismic methods, but it may provide additional information on the nature of the rocks of some basement domains. Therefore, deep rock bodies, particularly sub-horizontal layers, with low lateral magnetisation contrasts, typically remain unconstrained by magnetic modelling and resolution tests are necessary to evaluate the constraints on geological models. Geological models of Iberia and Newfoundland conjugate margins made of sub-horizontal layers only determined with magnetic modelling are unconstrained, and should not be used as robust results to infer rifting and COT processes, let alone to define conceptual models of magma-poor rifting.

5.1. The COT along IAM-9 in Iberia Abyssal Plain

Our new magnetic model along line IAM-9 (Figure 7) presents a structure integrating the available information from the Vp structure obtained with travel time tomography (Grevemeyer et al., 2022). The new magnetic model provides further constraints to the Vp model on (sub)vertical lithological boundaries, which are more accurately detected by magnetic data than sub-horizontal layers. Further, it provides complementary information on the nature of the rocks. Following the layer 2/3 Vp structure (Grevemeyer et al, 2022) we have modelled the basement with a layer 2 with higher magnetisation than in layer 3 (Figure 7), which is consistent with current conventional wisdom (Gee and Kent, 2007). The magnetic J-

ORIGINAL UNEDITED MANUSCRIPT

Downloaded from https://academic.oup.com/gji/advance-article/doi/10.1093/gji/ggad163/7120036 by Universidade do Porto user on 18 April 2023

anomaly is the oldest segment of the basement that can be fitted (amplitude and shape) with a classical oceanic crust structure, albeit with locally increased magnetisation, as discussed before. The basement structure to the west can be explained with a regular oceanic crust magnetisation. However, the segment to the east of the J-anomaly that had been modelled with magnetic data as oceanic crust (Russel and Whitmarsh, 2003; Minshull et al., 2014) has a Vp structure that does not conform the layer 2/3 typical of oceanic crust. Moreover, we show in Supplementary Text F and Supplementary Figure S6 that an eastward extension of oceanic crust is less compatible with the observed anomaly. Instead, we have modelled it as serpentinised exhumed mantle (Figure 7), partly overlaid by a basaltic layer related to J-anomaly ridge magmatic activity, an interpretation supported by multichannel seismic reflection images (Figure 8).

Therefore, the new magnetic model supports that the ~7 km thick basement of the J-anomaly represents an accreted oceanic structure directly abutting exhumed mantle, and further indicates that no clear layer 2/3 oceanic crust structure exists farther east. This structure, with the oldest oceanic crust represented by the J-anomaly directly in contact with exhumed mantle, is similar to the structure inferred from the Vp models of line FRAME-3 further south in the Iberia Abyssal Plain (Grevemeyer et al., 2022) and the line FRAME-2 in the Tagus Abyssal Plain (Merino et al., 2021a).

5.2.Implications for magma-poor rifting

The abrupt accretion of ~7 km of oceanic crust at breakup is at odds with the predictions of most conceptual and numerical 2D models of magma-poor COTs that infer a gradual input of

ORIGINAL UNEDITED MANUSCRIPT

Downloaded from https://academic.oup.com/gji/advance-article/doi/10.1093/gji/ggad163/7120036 by Universidade do Porto user on 18 April 2023

melt as the continental lithosphere thins and the asthenosphere progressively ascends. Most models infer the initial accretion of 2-3 km thick oceanic crust at breakup (e.g. Whitmarsh et al., 2001; Perez-Gussinye et al., 2006; Nirrengarten et al., 2017; Gillard et al., 2017). The J-anomaly oceanic crust is ~6 km thick in FRAME-P3 in the Iberia Abyssal Plain (Grevemeyer et al., 2022; Figure 1) and ~9 km thick in the Tagus Abyssal Plain (Merino et al., 2021a). Therefore, the breakup of West Iberia Margin, at least along the Tagus and Iberia Abyssal Plains, appears associated to the accretion of thicker-than-expected oceanic crust. One possible explanation is that the horizontal transition from initial 2-4 km to 6-9 km thick crust is rather fast and it is poorly defined in the Vp model along IAM-9. The better resolved Vp models of the FRAME lines might be compatible with a rapid transition from an initial ~4 km thick accretion (i.e. somewhat thicker than expected) to the 6-9 km thick igneous oceanic crust occurring in ~5-10 km along the lines (Merino et al., 2021a; Grevemeyer et al., 2022). However, the detailed structure of this transition is beyond the model resolution (Merino et al., 2021a), and could represent a narrow area of complex basaltic diking and sills into the edge of the COT basement.

An alternative explanation to the presence of 6-9 km thick igneous oceanic crust may instead be related to the propagation of a spreading center, requiring 3D interpretation of the evolution of the region. In this scenario, the transition into seafloor spreading crust could be abrupt as the amount of melting would not be directly related to local progressive continental lithospheric thinning. Although the potential time transgressive nature of the J-anomaly is discussed in previous papers, it has been related to magmatism during progressive rifting (e.g. Nirrengarten et al., 2017), and its significance for the relation between lithospheric thinning

ORIGINAL UNEDITED MANUSCRIPT

Downloaded from https://academic.oup.com/gji/advance-article/doi/10.1093/gji/ggad163/7120036 by Universidade do Porto user on 18 April 2023

and melt production was not recognized. In the Tagus Abyssal Plain (Figure 1), recent geophysical data revealed a complex lithospheric structure, with the exhumed mantle domain being interrupted seawards by a ribbon of continental lithosphere (Merino et al., 2021a) in a region previously interpreted as transitional (e.g. Sibuet et al., 2007), exhumed mantle (Bronner et al., 2011) or oceanic crust (e.g. Srivastava et al., 2000; Afilhado et al., 2008; Nirrengarten et al., 2017). The ribbon of continental lithosphere terminates seawards at the J-anomaly basement, which is interpreted to indicate that the first oceanic crust was accreted cutting a sector of the continental crust from the conjugate Newfoundland margin, and produced a jump in the locus of extension (Merino et al., 2021a).

The most likely geodynamic scenario is that the spreading centre was propagating northwards when cut a segment of continental crust in Tagus Abyssal Plain and cut exhumed mantle in the Iberia Abyssal Plain. This new scenario in which oceanic accretion is related to spreading centre (ridge) propagation, and not directly to progressive continental lithospheric thinning, could explain the abrupt change from the exhumed mantle of the COT to 6-9 km thick ocean crust. Previous studies put emphasis on models of rift propagation indicating that the end-of-rift age changes from the Tagus Abyssal Plain towards the Deep Galicia Margin, even though the age of breakup along the WIM is not well constrained by drill information (Whitmarsh and Miles, 1995; Tucholke and Sibuet, 2012). There are alternative conceptual models where seafloor spreading begins at the WIM when the rift system evolution connects the region of active extension to the spreading centre network and hot asthenosphere invades the rifting sub lithosphere region (e.g. Reston and Morgan, 2004). However, recent seismic studies of the Tagus Abyssal Plain show that the first oceanic crust created there is the J-anomaly and that it

ORIGINAL UNEDITED MANUSCRIPT

Downloaded from https://academic.oup.com/gji/advance-article/doi/10.1093/gji/ggad163/7120036 by Universidade do Porto user on 18 April 2023

does not coincide with the area of active mantle exhumation at the time (Merino et al., 2021a). The seismic data support that the northward propagation of the spreading center cut a sector of continental crust originally belonging to the Newfoundland conjugate rifted margin. That sector of continental crust is currently under the deep-water Tagus Abyssal Plain embedded between the oceanic J-anomaly crust and exhumed mantle (Merino et al., 2021a). Thus, the propagation was likely a 3D process that initiated at the Africa-America spreading center and cut across the paleo-plate boundary into the WIM, thereby linking the two systems, most likely disconnected from rift kinematics.

Similar geodynamic scenarios are feasible for the South China Sea where regional-scale spreading centre propagation is well established, and is proposed to have caused continental breakup and progressive rift-related extension to terminate from NE to SW along the basin (e.g. Cameselle et al., 2017; 2020). Such a geodynamic setting in which mantle melting may be driven by 3D processes may be difficult to assimilate in 2D evolutionary models from continental rifting to oceanic crust. The evolution of continental extension in several successive phases at the Iberia Abyssal Plain has been proposed (Peron-Pinvidic et al., 2007), but the large-scale 3D rift evolution and COT formation off West Iberia may have been overlooked, neglecting the implications for understanding the evolution of lithospheric extension, mantle exhumation and final breakup as onset of seafloor spreading.

5.3. Geophysical constraints on geological models

This study presents a detailed analysis of previous modelling efforts, as well as the evaluation of different proposed models and geological scenarios. We focus on the use of potential field

ORIGINAL UNEDITED MANUSCRIPT

Downloaded from https://academic.oup.com/gji/advance-article/doi/10.1093/gji/ggad163/7120036 by Universidade do Porto user on 18 April 2023

methods (magnetic) and its association with seismic data. But our claims that the resolution of the data sets must be carefully evaluated before using them as constraints for further modeling and interpretation applies to other types of data sets, with the risk of having unconstrained models being propagated in the literature. Moreover, as we show, methodologically incorrect results may be difficult to detect unless the geological model is carefully independently tested (Figure 2).

Our analysis indicates that potential field modelling to obtain the structure of physical properties of rifted margins needs to be used with caution. An unlimited number of geological models can explain potential field measurements, therefore additional constraints with complementary data must be used to justify a preferred model (Saltus and Blakely, 2011). A valuable argument is Occam's razor reasoning that calls for discarding complex models that include fine geological structure undetected with other methods. However, unnecessarily complex rifted margin models obtained with potential field modelling that either overvalue a perfect fit or provide a moderate fit of the anomaly data are not uncommon (e.g., Vijayan et al. 2013; Stanton et al., 2016; Szameitat et al., 2020). Potential field data modelling helps particularly to discriminate among possible interpretations of seismic data aiding to differentiate between lithologies of rocks (e.g. Prada et al., 2014; 2015; Neres et al., 2018; Merino et al., 2021b).

ORIGINAL UNEDITED MANUSCRIPT

Downloaded from https://academic.oup.com/gji/advance-article/doi/10.1093/gji/ggad163/7120036 by Universidade do Porto user on 18 April 2023

6. CONCLUSIONS

Magnetic data collected at sea-level cannot constrain, alone, the dimensions of sub-horizontal basement bodies at the COT under deep water and several km of sediment, as typical of rifted margins. Our results demonstrate the lack of constraints of several magnetic models of the Iberia-Newfoundland conjugate pair of margins that include unsupported complex geological structures.

We present a new magnetic model of the COT of the Iberia Abyssal Plain along the line IAM-9 constrained by new seismic data (Figure 7; Figure 8). The model supports that the J-anomaly basement is the oldest accreted oceanic crust of the West Iberia Margin. The high amplitude of the J-anomaly is best explained by a locally increased magnetisation, compared to normal oceanic crust.

The J-anomaly basement directly abuts exhumed mantle indicating an abrupt termination of mantle unroofing at the COT due to the accretion of ~6 km thick igneous oceanic crust, at the Iberia Abyssal Plain. Assuming that the J-anomaly is the first post breakup oceanic crust also in Tagus Abyssal Plain, as indicated by recent wide-angle seismic profiles, the first accretion of 6-9 km thick oceanic crust is at odds with predictions of conceptual and numerical models that generally anticipate a thinner crust. The transition from (2-4 km) thin to (6-9 km) thick crust could occur in 5-10 km along the cross section and perhaps the structures associated are below the resolution of current geophysical techniques.

Alternatively, the first igneous oceanic crust of early seafloor spreading was not formed by gradual mantle melting arising from progressive extension and thinning of continental

ORIGINAL UNEDITED MANUSCRIPT

Downloaded from https://academic.oup.com/gji/advance-article/doi/10.1093/gji/ggad163/7120036 by Universidade do Porto user on 18 April 2023

lithosphere. Instead, the 6-9 km thick oceanic crust structure could imply a sudden arrival of melt related to the three-dimensional evolution of the margin, where spreading center propagation may have terminated mantle exhumation causing the final breakup and the abrupt accretion of the J-anomaly crust.

7. ACKNOWLEDGEMENTS

We thank the constructive comments of Tim Minshull and one anonymous reviewer, and of the Editors Jenny Collier and Richard Holme, which led to significant improvement of the manuscript. We also thank Luis Matias (IDL-UL) for comments on a previous version of the manuscript. We thank Markku Pirttijärvi for making available the MAGPRISM software.

M. Neres acknowledges support from Fundação para a Ciência e Tecnologia, I.P./MCTES through national funds (PIDDAC) - projects LISA (PTDC/CTA-GEF/1666/2020), UIDB/50019/2020-IDL and PTDC/CTA-GEO/031885/2017. C.R. Ranero was supported by project FRAME (CTM2015-71766-R), ATLANTIS (PID2019-109559RB-I00), funded by the Spanish Ministry of Science and Innovation, and “Severo Ochoa Centre of Excellence” (CEX2019-000928-S) of the Spanish Research Agency (AEI). This is a contribution of the Grup de Recerca 2017 SGR 1662 “Barcelona Center for Subsurface Imaging” of the Generalitat de Catalunya.

ORIGINAL UNEDITED MANUSCRIPT

Downloaded from https://academic.oup.com/gji/advance-article/doi/10.1093/gji/ggad163/7120036 by Universidade do Porto user on 18 April 2023

8. DATA AVAILABILITY STATEMENT

Synthetic magnetic models were produced using the freely available MAGPRISM software (https://sites.google.com/view/markkussoftware/gravity-and-magnetic-software/magprism). Magnetic forward models were computed using the GMSYS modelling package of Oasis montaj™ from Seequent (research license).

9. REFERENCES

Afilhado, A., Matias, L., Shiobara, H., Hirn, A., Mendes-Victor, L., & Shimamura, H. (2008). From unthinned continent to ocean: The deep structure of the West Iberia passive continental margin at 38 N. Tectonophysics, 458(1-4), 9-50.

Barnett-Moore, N., Hosseinpour, M., Maus, S. (2016). Assessing discrepancies between previous plate kinematic models of Mesozoic Iberia and their constraints, Tectonics, 35, 1843–1862, doi:10.1002/2015TC004019

Barnett-Moore, N., Font, E., Neres, M. (2017). A Reply to the Comment on "Assessing Discrepancies Between Previous Plate Kinematic Models of Mesozoic Iberia and Their Constraints" by Barnett-Moore et al. Tectonics 36.12: 3286-3297

Blakely, R.J. (1996). Potential Theory in Gravity and Magnetic Applications. Cambridge Univ. Press, Cambridge

Boillot, G., Grimaud, S., Mauffret, A., Mougenot, D., Kornprobst, J., Mergoil-Daniel, J., & Torrent, G. (1980). Ocean-continent boundary off the Iberian margin: A serpentinite diapir west of the Galicia Bank. Earth Planet. Sci. Lett. 48, 23-34

ORIGINAL UNEDITED MANUSCRIPT

Downloaded from https://academic.oup.com/gji/advance-article/doi/10.1093/gji/ggad163/7120036 by Universidade do Porto user on 18 April 2023

Bronner, A., Sauter, D., Manatschal, G., Péron-Pinvidic, G., Munschy, M. (2011). Magmatic breakup as an explanation for magnetic anomalies at magma-poor rifted margins: Nature Geoscience, v. 4, 549–553, doi:10.1038/ngeo1201

Cameselle, A. L., Ranero, C. R., Franke, D., & Barckhausen, U. (2017) The continent-ocean transition on the northwestern South China Sea. Basin Research. https://doi.org/10.1111/bre.12137

Chazot, G., Charpentier, S., Kornprobst, J., Vannucci, R., Luais, B. (2005). Lithospheric mantle evolution during continental break-up: the West Iberia non-volcanic passive margin. Journal of Petrology 46, 2527–2568

Chenin, P., Manatschal, G., Ghienne, J. F., & Chao, P. (2021). The syn-rift tectono-stratigraphic record of rifted margins (Part II): A new model to break through the proximal/distal interpretation frontier. Basin Research

Christeson, G.L., J.A. Goff, R.S. Reece, (2019). Synthesis of oceanic crustal structure from two-dimensional seismic profiles. Reviews of Geophysics, 57, 504–529. https://doi.org/10.1029/2019RG000641

Dean, S.M., Minshull, T.A., Whitmarsh, R.B., Louden, K. (2000). Deep structure of the ocean–continent transition in the southern Iberia Abyssal Plain from seismic refraction profiles: The IAM9 transect at 40°20'N. J. Geophys. Res. 105, 5859–5886

Discovery 215 Working Group (1998). Deep structure in the vicinity of the ocean–continent transition zone under the southern Iberia Abyssal Plain, Geology, 26, 743–746

Gee, J.S., Kent, D.V. (2007). Source of oceanic magnetic anomalies and the geomagnetic polarity time scale. In Treatise on Geophysics 5.12 (ed Schubert, G.), 455-507

Godard, M., Lagabrielle, Y., Alard, O., & Harvey, J. (2008). Geochemistry of the highly depleted peridotites drilled at ODP Sites 1272 and 1274 (Fifteen-Twenty Fracture Zone, Mid-

ORIGINAL UNEDITED MANUSCRIPT

Downloaded from https://academic.oup.com/gji/advance-article/doi/10.1093/gji/ggad163/7120036 by Universidade do Porto user on 18 April 2023

Atlantic Ridge): Implications for mantle dynamics beneath a slow spreading ridge. Earth and Planetary Science Letters, 267(3-4), 410-425

Grevemeyer, I., Ranero, C.R., Ivandic, M. (2018). Structure of oceanic crust and serpentinization at subduction trenches. Geosphere 14 (2), 395–418

Grevemeyer, I., Ranero, C.R., Papenberg, C., Sallares, V., Bartolomé, R., Prada, M., Batista, L., Neres, M. (2022). The continent-to-ocean transition in the Iberia Abyssal Plain. Geology, 50(5), pp.615-619.

Haupert, I., G. Manatschal, A. Decarlis, P. Unternehr (2016). Upper-plate magma-poor rifted margins: Stratigraphic architecture and structural evolution, Marine and Petroleum Geology, 69, 241-261, doi.org/10.1016/j.marpetgeo.2015.10.020

Hidas, K., Varas-Reus, M. I., Garrido, C. J., Marchesi, C., Acosta-Vigil, A., Padron-Navarta, J. A., ... & Konc, Z. (2015). Hyperextension of continental to oceanic-like lithosphere: The record of late gabbros in the shallow subcontinental lithospheric mantle of the westernmost Mediterranean. Tectonophysics, 650, 65-79

Hjelt., S.-E. (1972). Magnetostatic anomalies of dipping prisms. Geoexploration 10, 239-254

Hopper, J. R., Dahl-Jensen, T., Holbrook, W. S., Larsen, H. C., Lizarralde, D., Korenaga, J., G. M. Kent, P. B. Kelemen (2003). Structure of the SE Greenland margin from seismic reflection and refraction data: Implications for nascent spreading center subsidence and asymmetric crustal accretion during North Atlantic opening. Journal of Geophysical Research: Solid Earth, 108(B5). https://doi.org/10.1029/2002JB001996

Lau, K. H., Louden, K. E., Funck, T., Tucholke, B. E., Holbrook, W. S., Hopper, J. R., & Christian Larsen, H. (2006). Crustal structure across the Grand Banks—Newfoundland Basin Continental Margin—I. Results from a seismic refraction profile. Geophysical Journal International, 167(1), 127-156

ORIGINAL UNEDITED MANUSCRIPT

Downloaded from https://academic.oup.com/gji/advance-article/doi/10.1093/gji/ggad163/7120036 by Universidade do Porto user on 18 April 2023

Maffione M, Morris, A., Plümper, O., van Hinsbergen, D.J.J. (2014). Magnetic properties of variably serpentinized peridotites and their implication for the evolution of oceanic core complexes. Geochemistry, Geophysics, Geosystems 15:923–944 https://doi.org/https://doi.org/10.1002/2013GC004993

Manatschal, G., Chenin, P., Ghienne, J. F., Ribes, C., & Masini, E. (2021). The syn-rift tectono-stratigraphic record of rifted margins (Part I): Insights from the Alpine Tethys. Basin Research, 34(1), 457-488

Merino, I., Prada, M., Ranero, C.R., Sallarès, V., & Calahorrano, A. (2021b) The structure of the continent- ocean transition in the Gulf of Lions from joint refraction and reflection travel-time tomography. Journal of Geophysical Research: Solid Earth, 126, e2021JB021711. https://doi. org/10.1029/2021JB021711

Merino, I., Ranero, C. R., Prada, M., Sallarès, V., & Grevemeyer, I. (2021a). The rift and continent-ocean transition structure under the Tagus Abyssal Plain West of the Iberia. Journal of Geophysical Research: Solid Earth, 126, e2021JB022629. https://doi. org/10.1029/2021JB022629

Minshull, T.A., Dean, S.M., Whitmarsh, R.B. (2014). The peridotite ridge province in the southern Iberia Abyssal Plain: Seismic constraints revisited. J. Geophys. Res. Solid Earth 119, 1580–1598

Müntener, O., & Manatschal, G. (2006). High degrees of melt extraction recorded by spinel harzburgite of the Newfoundland margin: The role of inheritance and consequences for the evolution of the southern North Atlantic. Earth and Planetary Science Letters, 252(3-4), 437-452

Müntener, O., & Manatschal, G. (2006). High degrees of melt extraction recorded by spinel harzburgite of the Newfoundland margin: The role of inheritance and consequences for the evolution of the southern North Atlantic. Earth and Planetary Science Letters, 252(3-4), 437-452

ORIGINAL UNEDITED MANUSCRIPT

Downloaded from https://academic.oup.com/gji/advance-article/doi/10.1093/gji/ggad163/7120036 by Universidade do Porto user on 18 April 2023

Neres, M., Font, E., Miranda, J. M., Camps, P., Terrinha, P., & Mirão, J. (2012). Reconciling Cretaceous paleomagnetic and marine magnetic data for Iberia: New Iberian paleomagnetic poles. Journal of Geophysical Research: Solid Earth, 117(B6)

Neres, M., Miranda, J.M. and Font, E. (2013). Testing Iberian kinematics at Jurassic-Cretaceous times. Tectonics, v. 32, 1312–1319. doi:10.1002/tect.20074

Neres, M., P. Terrinha, S. Custódio, S.M. Silva, J. Luis, J.M. Miranda (2018). Geophysical evidence for a magmatic intrusion in the ocean-continent transition of the SW Iberia margin. Tectonophysics, 744: 118-133. https://doi.org/10.1016/j.tecto.2018.06.014

Nirrengarten, M., Manatschal, G., Tugend, J., Kusznir, N. J., Sauter, D. (2017). Nature and origin of the J-magnetic anomaly offshore Iberia–Newfoundland: implications for plate reconstructions. Terra Nova 29, 20–28

Nirrengarten, M., Manatschal, G., Tugend, J., Kusznir, N., Sauter, D. (2018). Kinematic evolution of the southern North Atlantic: Implications for the formation of hyperextended rift systems. Tectonics, 37, 89–118. doi:10.1002/2017TC004495

Oufi, O., Cannat, M., Horen, H. (2002). Magnetic properties of variably serpentinized abyssal peridotites. Journal of Geophysical Research, 107(B5) doi:10.1029/2001jb000549

Pérez-Gussinyé, M., Morgan, J. P., Reston, T. J., Ranero, C. R. (2006). The rift to drift transition at non-volcanic margins: Insights from numerical modelling. Earth and Planetary Science Letters, 244(1-2), 458-473

Péron-Pinvidic, G., Manatschal, G., Minshull, T. A., Sawyer, D. S. (2007). Tectonosedimentary evolution of the deep Iberia-Newfoundland margins: Evidence for a complex breakup history. Tectonics, 26(2)

Peron-Pinvidic, G., Manatschal, G. and Osmundsen, P.T. (2013). Structural comparison of archetypal Atlantic rifted margins: A review of observations and concepts. Marine and petroleum geology, 43, pp.21-47

ORIGINAL UNEDITED MANUSCRIPT

Downloaded from https://academic.oup.com/gji/advance-article/doi/10.1093/gji/ggad163/7120036 by Universidade do Porto user on 18 April 2023

Peron-Pinvidic G, Manatschal G and the "IMAGinING RIFTING" Workshop Participants (2019) Rifted Margins: State of the Art and Future Challenges. Front. Earth Sci. 7:218. doi: 10.3389/feart.2019.00218

Hopper, J. R., T. Dahl-Jensen, W. S. Holbrook, H. C. Larsen, D. Lizarralde, J. Korenaga, G. M. Kent, and P. B. Kelemen, Structure of the SE Greenland margin from seismic reflection and refraction data: Implications for nascent spreading center subsidence and asymmetric crustal accretion during North Atlantic opening, J. Geophys. Res., 108(B5), 2269, doi:10.1029/2002JB001996, 2003

Pirttijärvi, Markku (2020 release). MAGPRISM software. https://sites.google.com/view/markkussoftware/gravity-and-magnetic-software/magprism

Prada, M., V. Sallares, C. R. Ranero, M. G. Vendrell, I. Grevemeyer, N. Zitellini, and R. de Franco (2014), Seismic structure of the Central Tyrrhenian basin: Geophysical constraints on the nature of the main crustal domains, J. Geophys. Res. Solid Earth,119, 52–70, doi:10.1002/2013JB010527.

Prada, M., V. Sallares, C. R. Ranero, M. G. Vendrell, I. Grevemeyer, N. Zitellini, and R. de Franco, (2015), The complex 3D transition from continental crust to back-arc magmatism and exhumed mantle in the Central Tyrrhenian rifted basin. 203(1):63-78 DOI: 10.1093/gji/ggv271 Geophys. J. International

Rampone, E., Hofmann, A.W. (2012). A global overview of isotopic heterogeneities in the oceanic mantle, Lithos, 148, 247-261

Reston, T. J.P. Morgan (2004). Continental geotherm and the evolution of rifted margins. Geology, 32 (2): 133–136. doi: https://doi.org/10.1130/G19999.1

Rovere, M., Ranero, C. R., Sartori, R., Torelli, L., & Zitellini, N. (2004). Seismic images and magnetic signature of the Late Juras- sic to Early Cretaceous Africa-Eurasia plate boundary

ORIGINAL UNEDITED MANUSCRIPT

Downloaded from https://academic.oup.com/gji/advance-article/doi/10.1093/gji/ggad163/7120036 by Universidade do Porto user on 18 April 2023

off SW Iberia. Geophysical Journal International, 158, 554–568. https://doi.org/10.1111/j.1365-246x.2004.02339.x

Russelll, S.M. and Whitmarsh, R.B. (2003). Magmatism at the West Iberia non-volcanic rifted continental margin: evidence from analyses of magnetic anomalies. Geophys. J. Int. 154 (3), 706–730

Sallarès, V., Martínez-Loriente, S., Prada, M., Gràcia, E., Ranero, C. R., Gutscher, M. A., et al. (2013). Seismic evidence of exhumed mantle rock basement at the Gorringe Bank and the adjacent Horseshoe and Tagus abyssal plains (SW Iberia). Earth and Planetary Science Letters, 365, 120–131. https://doi.org/10.1016/j.epsl.2013.01.021

Saltus, R. W., & Blakely, R. J. (2011). Unique geologic insights from" non-unique" gravity and magnetic interpretation. GSA Today, 21(12), 4-11.

Sandoval, L., Welford, J.K., MacMahon, H., Peace, A.L. (2019). Determining continuous basins across conjugate margins: The East Orphan, Porcupine, and Galicia Interior basins of the southern North Atlantic Ocean. Marine and Petroleum Geology, 110 , pp. 138-161.

Sawyer, D. S., Withmarsh, R. B., Klaus, A. (1994). and Shipboard Scientific Party. "Leg 149." In Proc. ODP, Init Rep., vol. 149, p. 719

Shillington, D. J. et al. (2006). Evidence for asymmetric nonvolcanic rifting and slow incipient oceanic accretion from seismic reflection data on the Newfoundland margin. J. Geophys. Res. 111, B09402

Sibuet, J.-C., Srivastava, S.P. and Spakman, W. (2004). Pyrenean orogeny and plate kinematics. J. Geophys. Res. Solid Earth, 109, B08104. doi: 10.1029/ 2003JB002514

Sibuet, J.-C., Srivastava, S., Manatschal, G. (2007). Exhumed mantle-forming transitional crust in the Newfoundland- Iberia rift and associated magnetic anomalies, J. Geophys. Res., 112, B06105, doi:10.1029/2005JB003856

ORIGINAL UNEDITED MANUSCRIPT

Downloaded from https://academic.oup.com/gji/advance-article/doi/10.1093/gji/ggad163/7120036 by Universidade do Porto user on 18 April 2023

Srivastava, S., Sibuet, J.-C., Cande, S., Roest, W., Reid, I. D. (2000). Magnetic evidence for slow seafloor spreading during the formation of the Newfoundland and Iberian margins, Earth Planet. Sci. Lett., 182, 61–76

Stanton, N., Manatschal, G., Autin, J., Sauter, D., Maia, M., & Viana, A. (2016). Geophysical fingerprints of hyper-extended, exhumed and embryonic oceanic domains: the example from the Iberia–Newfoundland rifted margins. Marine Geophysical Research, 37(3), 185-205.

Szameitat, L.S.A., Manatschal, G., Nirrengarten, M., Ferreira, F.J.F., Heilbron, M. (2020). Magnetic characterization of the zigzag shaped J-anomaly: Implications for kinematics and breakup processes at the Iberia– Newfoundland margins. Terra Nova 32, 369–380

Talwani, M. & Heirtzler, J.R. (1964). Computation of magnetic anomalies caused by two dimensional structures of arbitrary shape. In Computers in the Mineral Industries, Part 1, 464–480. Stanford Univ. Pub., Stanford

Tucholke, B.E. and Ludwig (1982). W.J. Structure and origin of the J-anomaly Ridge, western North Atlantic Ocean. J. Geophys. Res., 87(B11), 9389-9407

Tucholke, B., J.C. Sibuet (2012). Problematic plate reconstruction. Nature Geoscience 5, 676–677 (2012). https://doi.org/10.1038/ngeo1596

Tugend, J., Gillard, M., Manatschal, G., Nirrengarten, M., Harkin, C., Epin, M.E., Sauter, D., Autin, J., Kusznir, N. and Mcdermott, K. (2020). Reappraisal of the magma-rich versus magma-poor rifted margin archetypes. Geological Society, London, Special Publications, 476(1), pp.23-47.

Van Avendonk, H. J. A., Holbrook, W. S., Nunes, G. T., Shillington, D.J., Tucholke, B. E., Louden, K. E., Larsen, H.-C., and Hopper, J. R. (2006). Seismic velocity structure of the rifted margin of the eastern Grand Banks of Newfoundland, Canada, J. Geophys. Res., v. 111, B11404, doi:10.1029/2005JB004156

ORIGINAL UNEDITED MANUSCRIPT

Downloaded from https://academic.oup.com/gji/advance-article/doi/10.1093/gji/ggad163/7120036 by Universidade do Porto user on 18 April 2023

Varas-Reus, M. I., Garrido, C. J., Marchesi, C., Bodinier, J. L., Frets, E., Bosch, D., ... & Targuisti, K. (2016). Refertilization processes in the subcontinental lithospheric mantle: the record of the Beni Bousera orogenic Peridotite (Rif Belt, Northern Morocco). Journal of Petrology, 57(11-12), 2251-2270

Verhoef, J., Roest, W.R., Macnab, R., Arkani-Hamed, J., Members of the Project Team (1996). Magnetic anomalies of the Arctic and North Atlantic Oceans and Adjacent land areas, GSC Open file 3125. Geological Survey of Canada 225

Vijayan, V. R., Foss, C., & Stagg, H. (2013). Crustal character and thickness over the Dangerous Grounds and beneath the Northwest Borneo Trough. Journal of Asian Earth Sciences, 76, 389-398

Vissers, R.L.M. and Meijer, P.Th. (2012). Mesozoic rotation of Iberia: subduction in the Pyrenees? Earth Science Reviews 110, 93–110. doi:10.1016/j.earscirev.2011.11.001

Warren, J. M. (2016). Global variations in abyssal peridotite compositions. Lithos, 248, 193-219

White, R., and McKenzie, D. (1989), Magmatism at rift zones: The generation of volcanic continental margins and flood basalts, J. Geophys. Res., 94(B6), 7685– 7729, doi:10.1029/JB094iB06p07685.

Whitmarsh, R. B., and Miles, P. R. (1995). Models of the development of the West Iberia rifted continental margin at 40°30'N deduced from surface and deep-tow magnetic anomalies, J. Geophys. Res., 100(B3), 3789– 3806, doi:10.1029/94JB02877

Whitmarsh, R.B., Manatschal, G., and Minshull, T.A. (2001). Evolution of magma-poor continental margins from rifting to seafloor spreading: Nature, v. 413, p. 150–154.

Whitmarsh, R. B., Beslier, M. O., Wallace, P. J. (1998). "Leg 173." Proc. ODP, Init. Rep. Vol. 173

ORIGINAL UNEDITED MANUSCRIPT

Downloaded from https://academic.oup.com/gji/advance-article/doi/10.1093/gji/ggad163/7120036 by Universidade do Porto user on 18 April 2023

Geophysical Journal International

Supplementary Material for

An appraisal using magnetic data of the Continent to Ocean Transition Structure West of Iberia

Marta Neres[1,2], César R. Ranero[3,4]

[1] IPMA - Instituto Português do Mar e da Atmosfera, 1749-077 Lisboa, Portugal

[2] IDL - Instituto Dom Luiz, Universidade de Lisboa, 1749-016 Lisboa, Portugal

[3] ICM-CSIC - Consejo Superior de Investigaciones Científicas, Instituto de Ciencias del Mar, 08003 Barcelona, Spain

[4] ICREA -Institució Catalana de Recerca i Estudis Avançats, 08010 Barcelona, Spain

Corresponding author: Marta Neres (marta.neres@ipma.pt)

This file contains the following Supplementary Material:

- Supplementary Texts A-F
- Supplementary Figures S1-S6

A. Synthetic test on profile azimuth

Supplementary Figure S1 shows, for the edge effect calculations, the effect of changing the direction of the profile from W-E (as used for our synthetic tests) to 10°W (that compares to the 9°W trending of the IAM-9 profile). The effect is irrelevant: only a slight change in the shape of the anomalies is observed, and the general amplitude variation maintains.

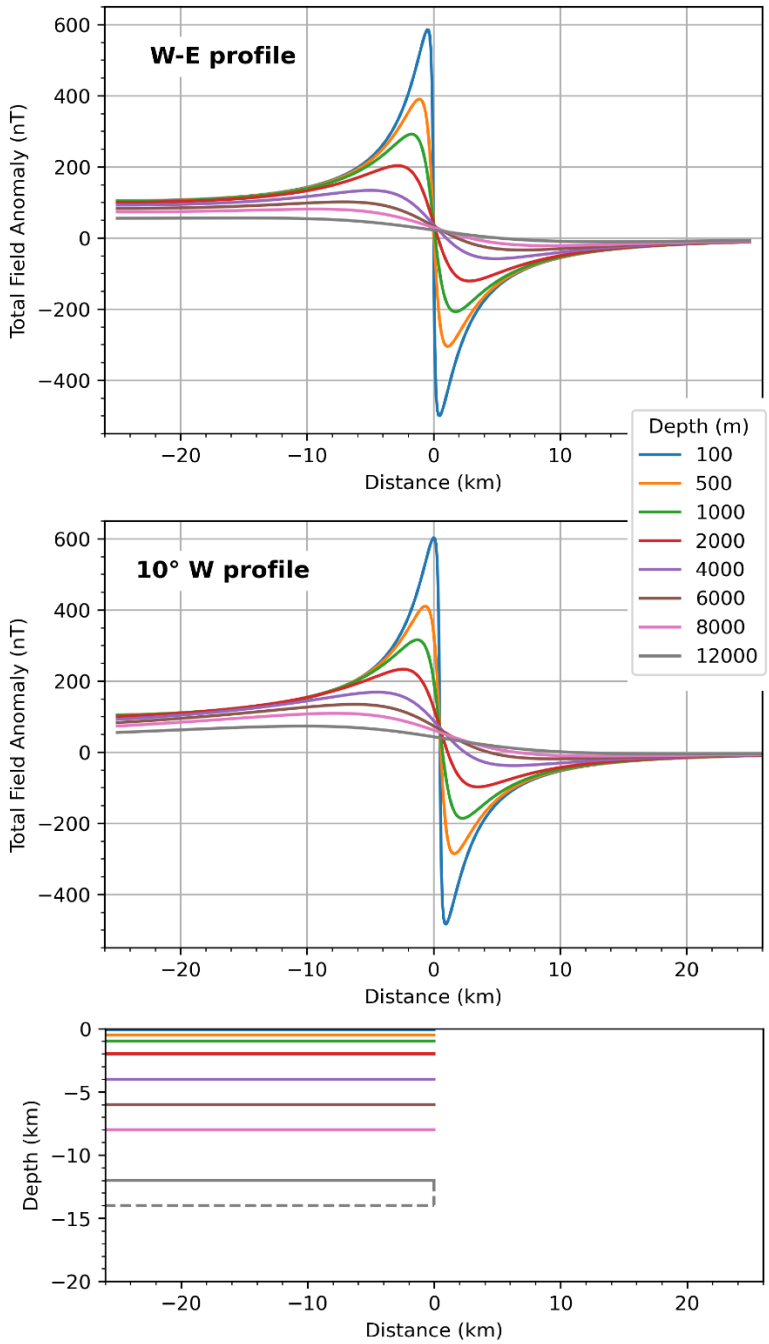

Supplementary Figure S1: Synthetic tests showing the effect of changing the trending direction of the profile from W-E (as presented in Figure 3) to 10°W (similar to IAM9 trending of 9°W).

B. Synthetic test on varying the inducing field declination

Magnetic modeling requires a correct definition of the local inducing field parameters, in order to get realistic calculated anomaly amplitudes. In this study, forward modeling of geological models (Figures 2, 4 and 7), made with GMsys, considered an IGRF-determined (at the time of survey) inducing field of 44 150 nT magnitude, 55.4° inclination and -7.4° declination.

For synthetic models, for simplicity, we consider declination = 0°, to allow the anomalies to be symmetric (once the profile is W-E) and thus focusing on the effect of the tested parameters.

Supplementary Figure S2 tests the effect, in the observed anomaly of the single magnetized body, of using declination values of 0°, -4°, and -8°. The main effect is a slight change in the symmetry of the anomaly, i.e., its western trough reaches more negative values and thus an increase in its total amplitude. For the 0.1 SI susceptibility, for instance, it represents an increase of about 8% in the anomaly value (between Dec=0 and Dec=-8).

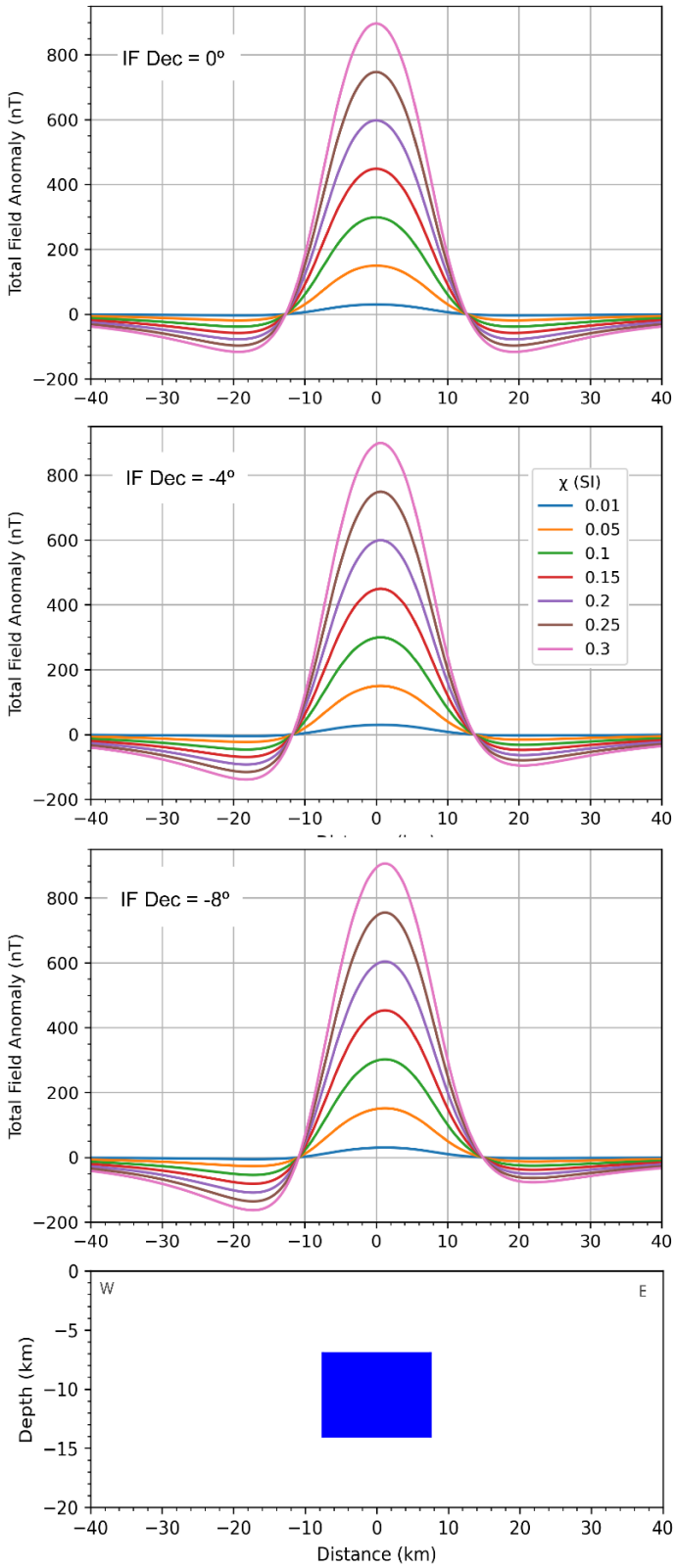

Supplementary Figure S2: Synthetic tests (similar to Figure 5 of the manuscript) for the magnetic anomaly of a single magnetized body considering different values for the inducing field declination: 0°, -4°, -8°. The inducing field magnitude (44 150 nT) and inclination (55.4°) are kept constant.

C. Synthetic test on layer thickness

Supplementary Figure S3 shows the results of a test with a series of bodies with the same top depth (7 km) and different thickness, so that their bottom reaches different depths. This test resembles the depth and geometry of the Iberia Abyssal Plain basement, thus being appropriate to evaluate the sensitivity to body thickness in the geometry tested.

Results show that increasing the layer thickness has a significant effect in the observed anomaly. Thus, the contribution of the deep part of magnetic layers cannot be disregarded and should, if possible, be constrained by independent methods.

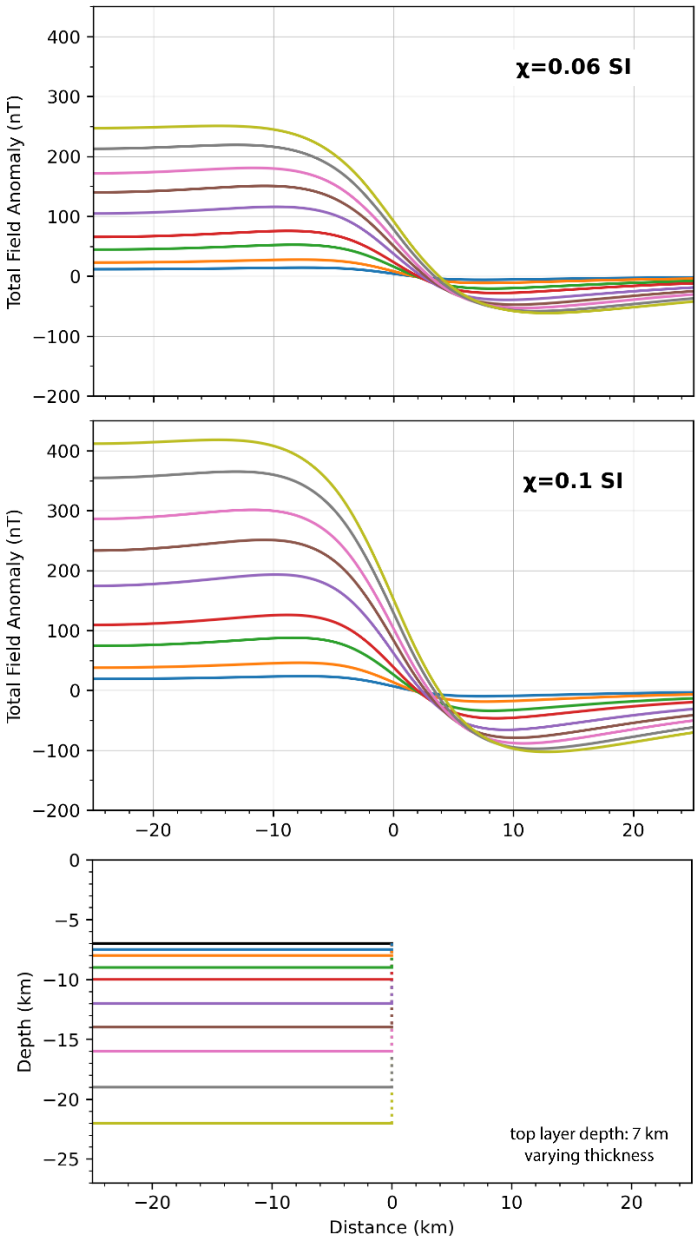

Supplementary Figure S3: Synthetic tests for the magnetic anomaly caused by the edge effect of magnetised layers with 7 km top depth and varying thickness (0.5 to 15 km thick), so that their bottom reaches different depths. The anomaly for a 2 km thick layer compares to the anomalies for 6 and 8 km deep in Figure 3.

D. Synthetic test on body width

Supplementary Figure S4 shows the variation of the magnetic anomaly with the width of a 7 km thick uniform body, extending in depth from 7 to 14 km, resembling the basement depth and thickness at Iberia Abyssal Plain.

For widths >30 km, the anomaly reveals the superposition effect of two edge anomalies from each side of the body (each of them equivalent to the 7 km thickness anomaly in Supplementary Figure 1), and the maximum amplitude is mostly the same. The maximum anomaly amplitude is achieved for a 20 km body width, and it rapidly decreases for widths <10 km.

Note that the 15 km wide body (dashed blue line) produces an anomaly equivalent to the anomaly in Figure 5 for χ = 0.1 SI. Also, this 15 km anomaly is similar to the anomaly in Figure 4b, even though the anomalies calculated with GMsys for geological models has a more complex shape.

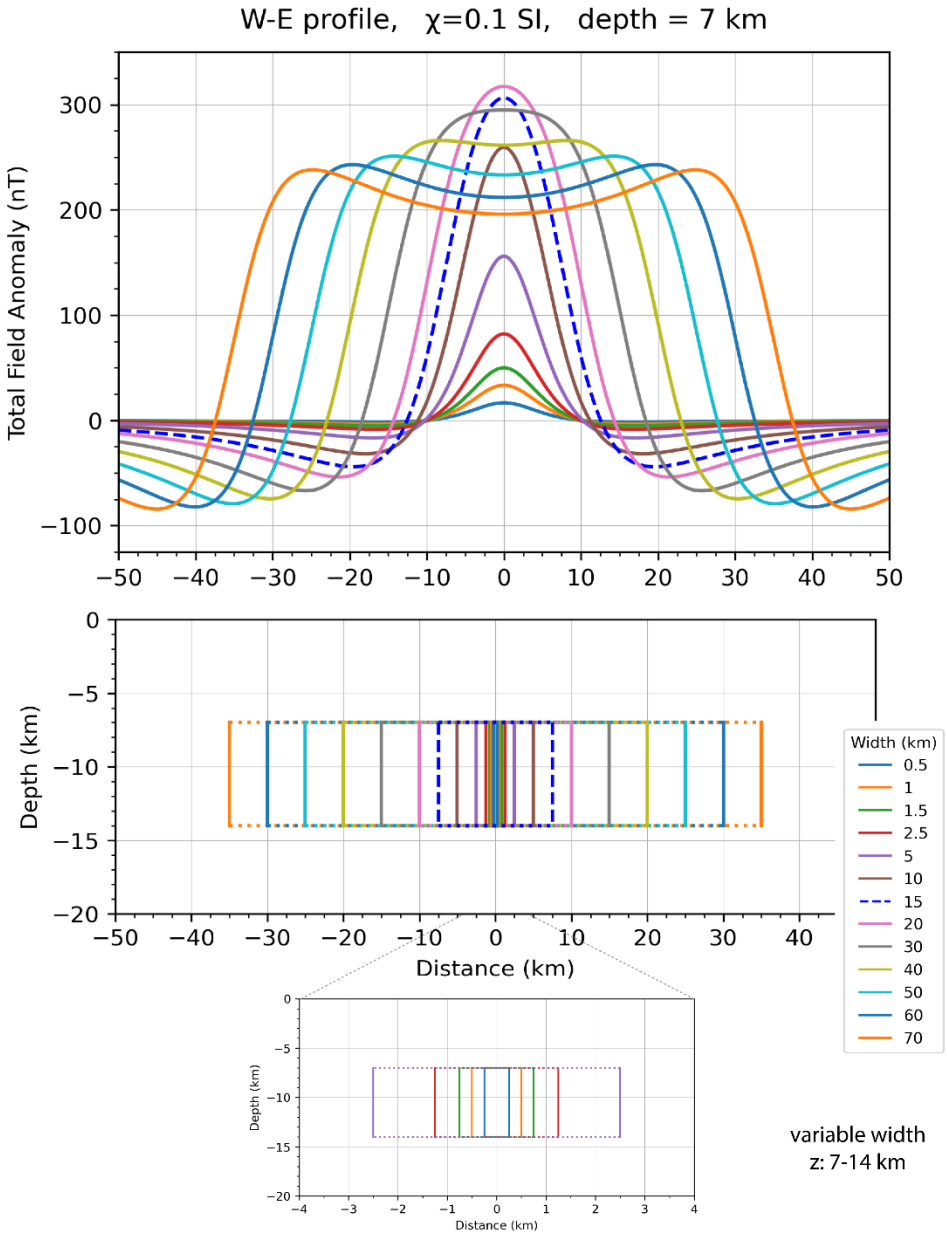

Supplementary Figure S4: Synthetic tests for the magnetic anomaly of a magnetised body with width varying from 0.5 to 70 km, constant thickness of 7 km, and fixed vertical limits extending from 7 to 14 km depth.

E. Definition of the base of oceanic layer 2

We built our preferred magnetic model for IAM-9 (Figure 7) by defining the magnetic layers based on the tomographic seismic velocity model. However, the seismically defined crustal structure may not coincide with the magnetic structure, leaving some degree of freedom to the definition of the geometry and to the assignment of parameters.

From the Vp point of view, for old oceanic crust the accepted Layer2/3 boundary is 6.5 km/s (e.g. Christeson et al., 2019). However, we use 6.0 km/s to define the base of the "basaltic crust" that has comparatively higher magnetisation compared to the lower crust, which is realistic. In other words, from 6.0 to 6.5 km/s we expect sheeted dikes with a lower magnetic signature, similar to gabbro.

Nonetheless, we have produced a magnetic model using 6.5 km/s to define the base of the magnetic layer 2 (instead of 6.0 km/s). We show this model in Supplementary Figure S5. The change in layer 2 turns it ≤2 km thick, while in the original Figure 7 layer 2 is ≤~1.2 km. A good fit of the anomaly amplitude is achieved by decreasing the magnetization of layer 2 from 13 Am^{-1} to 10 Am^{-1}, which is still a high magnetisation compared to regular oceanic crust (Gee and Kent, 2007).

Supplementary Figure S5 further supports that (reasonable) thickening of the source magnetic layer with a regular magnetisation (e.g. 5 Am^{-1}) would not be able to fit the observed anomaly, so that a comparatively high magnetisation appears unavoidable.

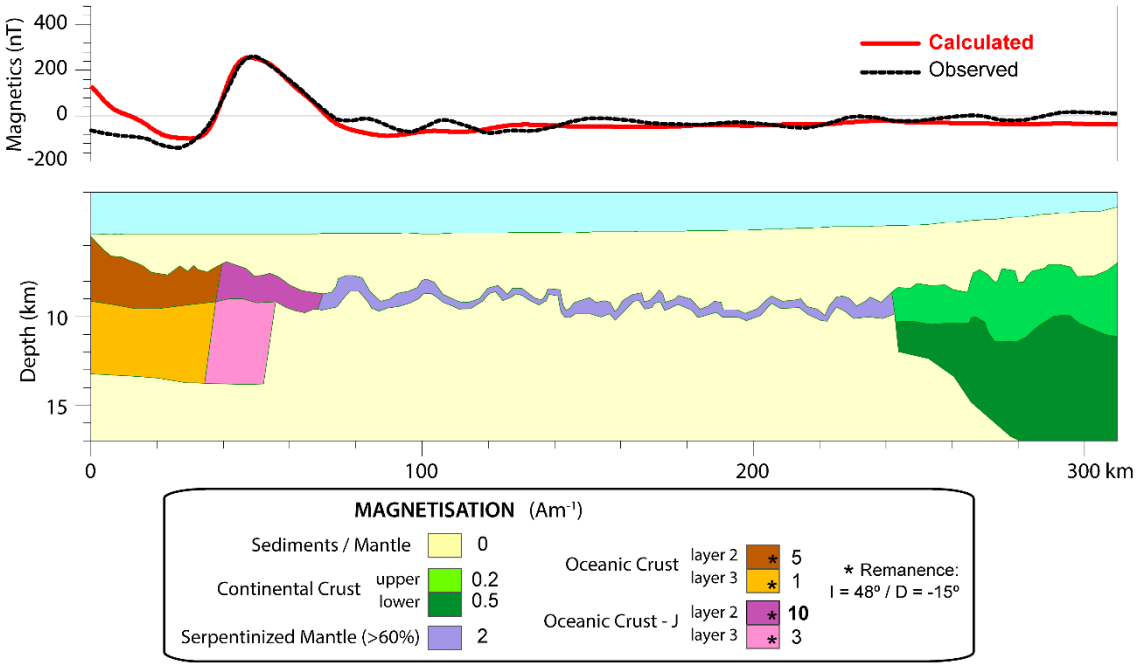

Supplementary Figure S5: Modified magnetic model, considering Vp~6.5 km/s for defining the layer 2 - layer 3 limit at oceanic crust, thus increasing the layer 2 thickness. The observed data can be fit by decreasing the magnetisation of layer 2 to 10 Am^{-1}, still a high magnetisation compared to regular oceanic crust.

F. Definition of the east (landward) limit of oceanic crust

We compare our preferred model (Figure 7; Supplementary Figure S6a) to models considering alternative boundaries between the exhumed mantle and the oceanic crust. Two possible alternative models are presented in Supplementary Figure S6b-c to test the potential of the landward extension of the oceanic crust, as proposed by Minshull et al. (2014).

Supplementary Figure S6b model extends normal (Layer2/3) oceanic structure further to the east (Minshull et al., 2014) with a corresponding normal magnetisation. The model produces a mostly symmetric anomaly that does not explain comparatively well the asymmetric slopes of the observed J-anomaly.

Supplementary Figure S6c model uses increased magnetisation for the crust extended to the east, following the magnetic signature of the J crust on the preferred model, but the broad resulting anomaly that does not explain well the J-anomaly.

Our preferred model (Supplementary Figure S6a) has an asymmetric structure of the magnetic source able to produce the observed anomaly. The extension of the upper oceanic layer to the east is supported by the seismic image along profile IAM-9 (Figure 8).

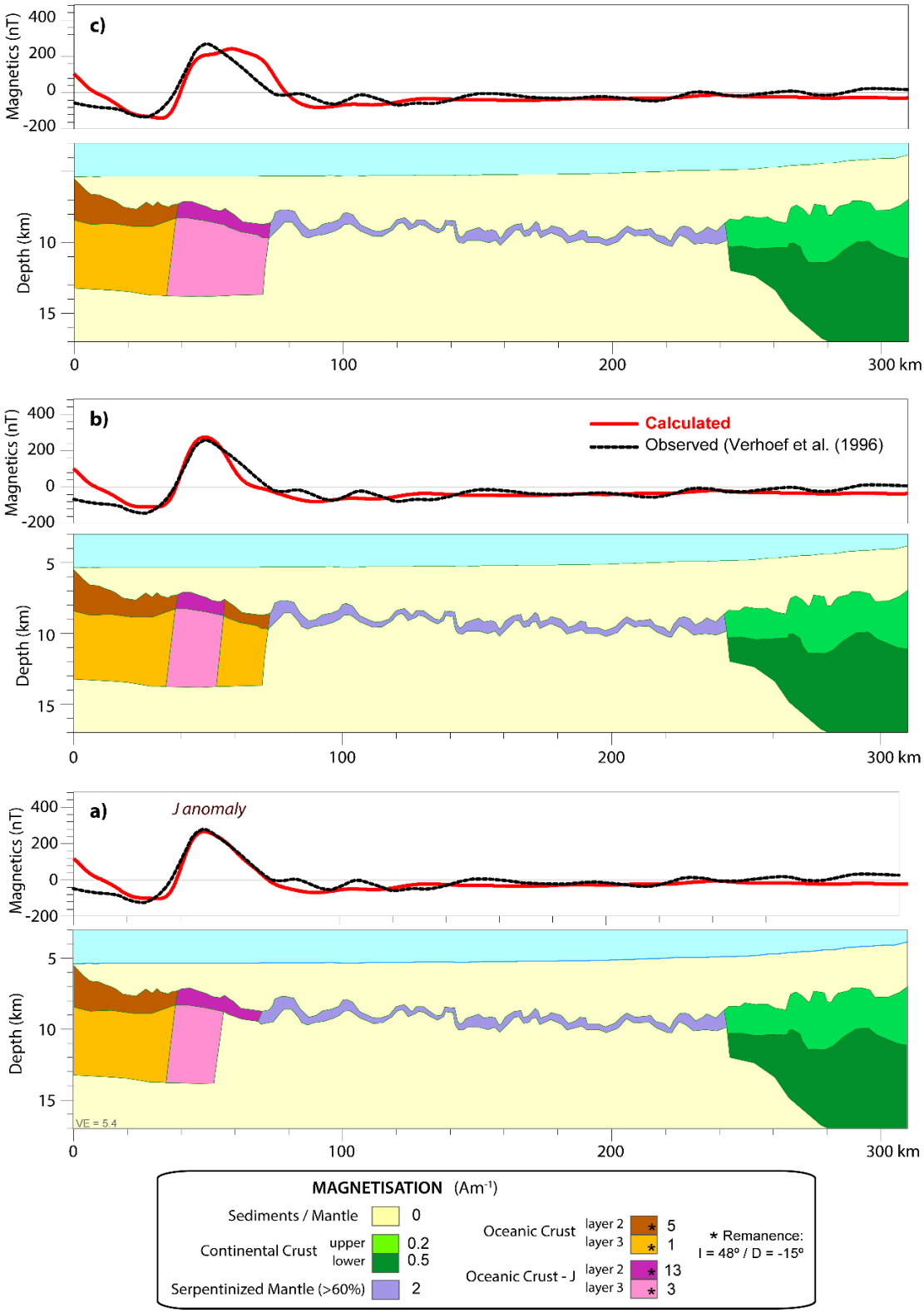

Supplementary Figure S6: Magnetic models testing an alternative eastern limit for the oceanic crust. (a) Magnetic model of Figure 7 (preferred model); (b) High magnetization sector limited to J block and regular magnetization crust extending eastward to the limit proposed by Minshull et al (2014) (dashed line in Figure 6b); (c) J-type high magnetization layers extending eastwards.